

Clustering-aware Graph Construction: A Joint Learning Perspective

Yuheng Jia, Hui Liu, Junhui Hou, *Member, IEEE*, and Sam Kwong, *Fellow, IEEE*,

Abstract—As a promising clustering method, graph-based clustering converts the input data to a graph and regards the clustering as a graph partition problem. However, traditional graph clustering methods usually suffer from two main limitations: *i*), graph clustering is a feed-forward process, and cannot make use of the information from clustering result, which is more discriminative than the original graph; and *ii*), once the graph is constructed, the clustering process is no longer related to the input data, which may neglect rich information of raw features. To solve the above defects, we propose to learn the similarity graph adaptively, which compromises the information from the raw features, the initial graph and the clustering result. And thus, the proposed model is naturally cast as a joint model to learn the graph and generate the clustering result simultaneously, which is further efficiently solved with convergence theoretically guaranteed. The advantage of the proposed model is demonstrated by comparing with 19 state-of-the-art clustering methods on 10 datasets with 4 clustering metrics.

Index Terms—Adaptive graph learning, Graph Clustering, KKT conditions.

I. INTRODUCTION

As a fundamental task in machine learning, clustering aims to partition input data into different groups, where one sample is more similar to a sample in the same group than a sample from different groups. Many real-world applications can be formulated as a clustering problem, e.g., image segmentation [1], [2], image classification [3], community detection [4], recommender system [5], tumor discovery [6], [7], [8], and data visualization [9]. To partition the data, many clustering methods were proposed like K-means, Gaussian mixture models (GMM) [10], mean shift [11], [12], and various graph-based clustering methods [13], [14], [15], [16], [17].

Different from K-means based methods that perform clustering on the raw input, graph based methods first transform raw features to a similarity graph, and then partition the graph into different subgraphs. However, graph partition is generally challenging to solve due to its NP-hardness [18]. To remedy this problem, many approximate solutions were proposed [13], [14], [17], which is called graph clustering. The representative

graph clustering method includes various spectral clustering (SC) methods [13], [14], [17] and symmetric nonnegative matrix factorization (SymNMF) [15], [16]. They distinguish each other with different relaxation methods or decomposition methods. See section II-B for the detailed comparison.

How to build a reasonable graph plays the critical role in graph clustering, since its quality usually determines the final clustering performance. The most-well known graph construction methods is p -nearest-neighbor graph that connects a sample with its top p nearest samples with non-negative weights to measure their similarities, and assigns 0 to the non-connect samples. This naive construction method may produce limited performance due to the fact that it is not robust to various noise [19]. To solve this problem, many advanced graph construction models were proposed [19], [20], [21], [22], [23], [24], [24], [3]. See the detailed review in section II-B. Although they have been applied to many applications, it is still not clear whether the constructed graph fits the task of clustering or not. They reason is that they usually treat clustering as a three-step process, i.e., first construct a graph, second embed the graph into a reduced dimension space (like spectral embedding), and third partition the embedding through post-processing like K-means.

To address the above problems, in this paper we propose a clustering model that can simultaneously divide the data into different clusters and construct graph. Specifically, we argue graph construction should explore information from the following three views: *i*) the initial similarity graph, which is usually practical in many applications; *ii*), the raw features, which usually prove rich information and has been overlooked by a traditional graph clustering method; and *iii*), the clustering result, which is usually more discriminative than the input graph. Moreover, inherit from SymNMF, the proposed model can directly generate the clustering membership matrix without post-processing. Consequently, the proposed model unifies graph construction and data partition into a joint model to exploit the mutual enhancement relation between them, where a more global solution can be obtained and the learned graph may be more fitted with clustering task. It is worth pointing out that formulating two correlate tasks into a joint optimization framework to mutually enhance each other has been proven to be effective in many works [3], [25], [26], [27], [28], [29], [30], [29]. The proposed model is finally formulated as a nonnegative and off-diagonal¹ constrained optimization problem, which is solved efficiently in an iterative manner

Y. Jia and H. Liu are with the Department of Computer Science, City University of Hong Kong, Kowloon, Hong Kong, (e-mail: yuheng.jia@my.cityu.edu.hk; hliu99-c@my.cityu.edu.hk).

S. Kwong and J. Hou are with the Department of Computer Science, City University of Hong Kong, Kowloon, Hong Kong and also with the City University of Hong Kong Shenzhen Research Institute, Shenzhen, 51800, China, (e-mail: cssamk@cityu.edu.hk; jh.hou@cityu.edu.hk).

This work was supported in part by the Natural Science Foundation of China under Grants 61772344, 61672443, 61873142 and in part by Hong Kong RGC General Research Funds 9042489 (CityU 11206317), 9042322 (CityU 11200116), and Early Career Scheme Funds 9048123 (CityU 21211518).

¹the learned similarity matrix should be an off-diagonal matrix to avoid the trivial solution.

with convergence theoretically guaranteed. By comparing the proposed models with 19 state-of-the-art clustering methods on 10 commonly used datasets with 4 different clustering metrics, the effectiveness of the proposed model is validated. In addition, improvement of the proposed model is confirmed by the Wilcoxon rank sum test at a significance level of 0.05.

The main contributions of this paper are summarized as follows:

1. The proposed method simultaneously learns a clustering membership matrix and a graph matrix, which can exploit the mutual enhancement relation between the two separate steps and lead to a more global solution.
2. The adopted graph is constructed by exploring the complementary information from the predefined similarity graph (view 1), the raw features (view 2) and the discriminative clustering result (view 3).
3. The proposed optimization method has the following theoretical guarantees: *i*), the constraints in the proposed model can be naturally satisfied² along with the optimization process; *ii*), each optimization step can decrease the objective function value; and *iii*), the converged limit point is a stationary point that satisfies the Karush-Kuhn-Tucker (KKT) conditions.

This paper is organized as follows. In section II, we discuss the related works. Section III presents the proposed model, the optimization method, its theoretical guarantees and the computational complexity analysis. Experimental comparisons and analyses are shown in section IV, and finally section V concludes this paper.

II. RELATED WORK

Before introducing the related works, we first give the notations of this paper. Matrices are denoted by boldface uppercase letters, e.g., \mathbf{A} , and element at the i th row and j th column of a matrix is denoted as $\mathbf{A}_{i,j}$ or $a_{i,j}$. Vectors are represented by boldface lowercase letters, e.g., \mathbf{a} and scales are represented by italic lowercase letters, e.g., a . Moreover, \top stands for the transpose of a matrix, $\|\mathbf{A}\|_F = \sqrt{\sum_i \sum_j \mathbf{A}_{i,j}^2}$ is the Frobenius norm of matrix \mathbf{A} , $\text{diag}(\cdot)$ returns the diagonal elements of a matrix as a vector, \odot returns the Hadamard product of two matrices, i.e., the element-wise multiplication of two matrices, $\exp(\cdot)$ returns the exponential value, $\langle \cdot, \cdot \rangle$, calculates the inner product of two matrices, \mathbf{I}_k denotes an identity matrix of size $k \times k$, and $\mathbf{A} \geq 0$ means each element of \mathbf{A} is greater than or equal to 0, i.e., $\mathbf{A}_{i,j} \geq 0, \forall i, j$.

A. Clustering

Clustering aims to partition a set of samples into different groups according to their similarities, where samples in the same group are close to each other while samples from the different groups are dissimilar to each other. Taking one of the most-well known clustering methods K-means as an example, let $\mathbf{X} = \{\mathbf{x}_1, \mathbf{x}_2, \dots, \mathbf{x}_n\} \in \mathbb{R}^{d \times n}$ denote the input data, where n is the total sample amount, $\mathbf{x}_i \in \mathbb{R}^{d \times 1}$ represents the

i th sample and d is the number of features for each sample, K-means mathematically solves the following optimization problem,

$$\min_{\mathbf{Y} \mathbf{1} = \mathbf{1}, \mathbf{Y} \in \text{Ind}, \mathbf{Y} > 0, \mu_j} \sum_{i=1}^n \sum_{j=1}^c \mathbf{Y}_{i,j} \|\mathbf{x}_i - \mu_j\|_2^2, \quad (1)$$

where $\mathbf{Y} \in \text{Ind}$ means \mathbf{Y} is a clustering indicator matrix, μ_j is the centroid of the j th cluster. K-means seeks a hard partition for the input data, a more flexible method termed fuzzy K-means [29] was proposed that can generate a soft assignment matrix, i.e.,

$$\min_{\mathbf{Y} \mathbf{1} = \mathbf{1}, \mathbf{Y} \geq 0, \mu_j} \sum_{i=1}^n \sum_{j=1}^c \mathbf{Y}_{i,j} \|\mathbf{x}_i - \mu_j\|_2^2. \quad (2)$$

B. Graph Clustering

Although K-means can be solved efficiently, it usually cannot partition the non-spherical distributed samples correctly. To solve this problem, many graph clustering methods were proposed [15], [13]. Different from traditional clustering methods that partition the raw features \mathbf{X} straightforwardly, graph clustering transform the data clustering as a graph partition problem. Specifically, a typical graph clustering method is composed of the following steps:

1. Given \mathbf{X} , generate an affinity graph matrix $\mathbf{G} \in \mathbb{R}^{n \times n}$ to represent \mathbf{X} , where entries in \mathbf{G} denote the similarities between corresponding samples.
2. Decompose the normalized affinity matrix (also known as Laplacian matrix) to generate the low-dimensional embedding.
3. Obtain the clustering membership according to the embedding.

In the following, we will briefly discuss the commonly and recently used approaches for each steps.

1) *Graph construction*: The most commonly used graph is p -nearest-neighbor (p NN) graph [18] that only connects a specified sample with its top p nearest samples under some distance metrics. Specifically,

$$\mathbf{G}_{ij} = \begin{cases} \mathcal{G}_{ij} & \mathbf{x}_j \in \mathcal{P}(\mathbf{x}_i) \\ 0 & \text{otherwise,} \end{cases} \quad (3)$$

where $\mathcal{P}(\mathbf{x}_i)$ indicates the top p nearest samples of \mathbf{x}_i , and \mathcal{G}_{ij} is the weight between \mathbf{x}_i and \mathbf{x}_j . The binary weighting strategy simply sets $\mathcal{G}_{ij} = 1$ for the connected samples. Another more commonly adopted approach is to set the weights according to a radial basis function kernel (RBF), i.e.,

$$\mathcal{G}_{ij} = \exp\left(-\frac{\|\mathbf{x}_i - \mathbf{x}_j\|_2^2}{\sigma^2}\right) \quad (4)$$

to preserve the similarity relations between the connected samples, where σ^2 is the band width of the RBF kernel. Another commonly used graph construction method is ϵ -neighborhood graph that connects a certain sample with other samples within a ball of radius ϵ .

Both p NN and ϵ -neighborhood graphs are sensitive to the outliers and noises. To solve this problem, many advanced

²i.e., non-negativity for all the variables and off-diagonal for the similarity matrix.

learning methods were proposed to construct the graph weight matrix recently. For example, Cheng *et al.* [19] proposed to learn an ℓ^1 graph based on the automatic sparsity property of the ℓ_1 norm; many subspace segmentation methods use the self-representative property to build a similarity graph [20], [21], [22]; and Nie *et al.* [23] proposed to learn the neighbors of a specific sample adaptively; [24], [24] learned the graph from the perspective of graph signal processing. Wu *et al.* [3] constructed a discriminative graph with the guidance of the supervisory information.

2) *Embedding*: Given \mathbf{W} , graph clustering decomposes \mathbf{W} to generate a lower-dimensional embedding. For example, SC [13] formulate graph clustering as a spectral decomposition problem,

$$\min_{\mathbf{V}} \|\mathbf{W} - \mathbf{V}\mathbf{V}^T\|_F^2, \text{ s.t.}, \mathbf{V}\mathbf{V}^T = \mathbf{I}_k, \quad (5)$$

where $\mathbf{V} \in \mathbb{R}^{k \times n}$ is the reduced dimension embedding and can be calculated by the spectral decomposition of \mathbf{W} . As an alternative, SymNMF [16], [15] decomposes the Laplacian matrix to the product of two nonnegative matrices,

$$\min_{\mathbf{V}} \|\mathbf{W} - \mathbf{V}\mathbf{V}^T\|_F^2, \text{ s.t.}, \mathbf{V} \geq 0, \quad (6)$$

to produce the lower-dimensional embedding. Other advanced methods like sparse SC (SSC) [31] seeks a block diagonal appearance of $\mathbf{V}\mathbf{V}^T$, and nonnegative spectral clustering (NSC) [14] generate an orthogonal nonnegative embedding.

3) *Generation of the clustering indicator matrix*: Since the lower-dimensional embedding in graph clustering usually can not indicate the clustering membership, traditionally post-processing like K-means should be carried out to obtain the final cluster indicator result. As a special case, SymNMF generates a nonnegative embedding and the position of the largest value in the i th column can indicate the clustering membership of \mathbf{x}_i .

III. PROPOSED MODEL

A. Model Formulation

As aforementioned, the quality of graph determines the performance of a graph clustering method. However, it is quite challenging to judge whether the initial graph is good enough or not. To solve this problem, we propose to learn a graph in the clustering process adaptively. Intuitively, the following information can contribute to the construction of similarity graph:

- 1, The learned similarity graph should approximate the initial graph, since the initial one is usually useful in practical applications.
- 2, The raw features can provide rich information on constructing the similarity graph matrix.
- 3, Since an imperfect similarity graph can produce a perfect cluster indicator matrix, which means the generated parathion is more discriminative than the original graph, clustering result is also useful in constructing similarity graph.

Assume the initial graph matrix is denoted by \mathbf{W} , and the to be learned similarity graph is denote as $\mathbf{S} \in \mathbb{R}^{n \times n}$, the first rule can be mathematically expressed as

$$\min_{\mathbf{S}} \|\mathbf{S} - \mathbf{W}\|_F^2. \quad (7)$$

When the minimum of Eq. (7) is obtained, the learned \mathbf{S} is identical to the initial similarity graph \mathbf{W} .

For the second rule, we adopt a self-expressive model [22] to explore the information from raw features, i.e.,

$$\min_{\mathbf{S}} \|\mathbf{X} - \mathbf{X}\mathbf{S}\|_F^2 + \|\mathbf{S}\|_F^2, \text{ s.t.}, \mathbf{S} \geq 0, \text{diag}(\mathbf{S}) = 0, \quad (8)$$

where $\text{diag}(\mathbf{S}) = 0$ removes the trivial solution that $\mathbf{S} = \mathbf{I}_n$. Peng et.al. [22] theoretically indicates that a self-representation model with Frobenius norm enjoys the property of intra-subspace projection dominance (IPD), i.e., the coefficients over intra subspaces data points are larger than those over inter-subspace data. Based on IPD, we can expect that \mathbf{S}_{ij} for samples from the same subspace will have higher value.

According to the third rule, \mathbf{S} can also gain information from the cluster membership matrix, i.e.,

$$\min_{\mathbf{V}, \mathbf{S}} \|\mathbf{S} - \mathbf{V}\mathbf{V}^T\|_F^2 \\ \text{s.t.}, \mathbf{V} \geq 0, \quad (9)$$

where $\mathbf{V} \in \mathbb{R}^{n \times c}$ is a clustering membership matrix like SymNMF, Note that both the cluster indicator matrix \mathbf{V} and similarity matrix \mathbf{S} are the to be optimized variables in Eq. (9), which is different from the objective function of SymNMF in Eq. (6) that only learns the clustering indicator matrix.

Combing all the components together, the proposed model is finally formulated as

$$\min_{\mathbf{V}, \mathbf{S}} \|\mathbf{S} - \mathbf{V}\mathbf{V}^T\|_F^2 + \alpha \|\mathbf{X} - \mathbf{X}\mathbf{S}\|_F^2 + \beta \|\mathbf{S} - \mathbf{W}\|_F^2 \\ \text{s.t.}, \mathbf{V} \geq 0, \mathbf{S} \geq 0, \text{diag}(\mathbf{S}) = 0, \quad (10)$$

where \mathbf{S} is the adaptive similarity matrix and \mathbf{V} is the learned clustering indicator. From Eq. (10) we can see that the proposed model constructs the similarity matrix by exploiting the following information: the predefined similarity matrix, the raw features and the clustering result. Note that $\|\mathbf{S}\|_F^2$ in Eq. (8) is absorbed in $\|\mathbf{S} - \mathbf{W}\|_F^2$ in Eq. (10) to reduce the number of regularization terms. It is also worth pointing out that each view is constructed straightforwardly without extra processing. Moreover, since the predefined similarity matrix \mathbf{W} is usually a sparse one, only a few entries of \mathbf{S} will be remarkably larger than 0 by minimizing $\|\mathbf{S} - \mathbf{W}\|_F^2$. Together with the IPD property, we can hope only the connections within the same subspace will be kept. In addition, inherit from SymNMF, \mathbf{V} can act as a clustering membership matrix, where the location of the maximum value of the i th row of \mathbf{V} indicates the clustering membership of \mathbf{x}_i . Note that for a traditional SC method, additional post-processing like K-means is required to obtain the final clustering result.

From another perspective, Eq. (10) formulates graph learning (i.e., \mathbf{S}) and clustering (i.e., \mathbf{V}) into a joint model to exploit the relation between them and mutually enhance each other. While the traditional graph clustering [20], [21], [22] methods usually implement the same task by a three-step manner that

first construct a similarity matrix, then decompose the graph into a reduced-dimension space, and finally perform clustering on that low dimension embedding, where the solution of each task is sub-optimal.

B. Optimization Method

To solve Eq. (10), we first introduce the Lagrangian function as

$$\mathcal{L}(\mathbf{S}, \mathbf{V}, \Phi, \Psi) = \mathcal{O}(\mathbf{V}, \mathbf{S}) - \langle \Phi, \mathbf{S} \rangle - \langle \Psi, \mathbf{V} \rangle, \quad (11)$$

where $\Phi \in \mathbb{R}^{n \times n} \geq 0$ and $\Psi \in \mathbb{R}^{c \times n} \geq 0$ are Lagrangian multiplier matrices and $\mathcal{O}(\mathbf{V}, \mathbf{S})$ denotes the objective function. Following the KKT condition, the optimal solution of Eq. (10) also makes the derivatives of $\mathcal{L}(\mathbf{S}, \mathbf{V}, \Phi, \Psi)$ with respect to \mathbf{S} and \mathbf{V} be 0, i.e.,

$$\frac{\partial \mathcal{L}}{\partial \mathbf{S}} = 2(\mathbf{S} - \mathbf{V}\mathbf{V}^\top) + 2\alpha \mathbf{X}^\top (\mathbf{X}\mathbf{S} - \mathbf{X}) + 2\beta(\mathbf{S} - \mathbf{W}) - \Phi = \mathbf{0}, \quad (12)$$

and

$$\frac{\partial \mathcal{L}}{\partial \mathbf{V}} = -2(\mathbf{S}\mathbf{V} + \mathbf{S}^\top \mathbf{V}) + 4\mathbf{V}\mathbf{V}^\top \mathbf{V} - \Psi = \mathbf{0}, \quad (13)$$

where $\mathbf{0}$ is an all zeros matrix with proper size. From the KKT complementary slackness conditions $\Phi_{ij} \mathbf{S}_{ij}^2 = 0$, $\Psi_{ij} \mathbf{V}_{ij}^4 = 0$, $\forall i, j$, we obtain the following updating equations for \mathbf{S} and \mathbf{V} , respectively, i.e.,

$$\mathbf{S}_{ij} = \mathbf{S}_{ij} \left(\frac{(\mathbf{V}\mathbf{V}^\top + \alpha(\mathbf{X}^\top \mathbf{X})^+ + \alpha(\mathbf{X}^\top \mathbf{X})^- \mathbf{S} + \beta \mathbf{W})_{ij}}{(\mathbf{S} + \alpha(\mathbf{X}^\top \mathbf{X})^+ \mathbf{S} + \alpha(\mathbf{X}^\top \mathbf{X})^- + \beta \mathbf{S})_{ij}} \right)^{\frac{1}{2}}, \quad (14)$$

and

$$\mathbf{V}_{ij} = \mathbf{V}_{i,j} \left(\frac{(\mathbf{S}\mathbf{V} + \mathbf{S}^\top \mathbf{V})_{ij}}{(2\mathbf{V}\mathbf{V}^\top \mathbf{V})_{ij}} \right)^{\frac{1}{4}}, \quad (15)$$

where $(\mathbf{X}^\top \mathbf{X})^+$ and $(\mathbf{X}^\top \mathbf{X})^-$ separate the positive and negative elements of $\mathbf{X}^\top \mathbf{X}$ ³, i.e.,

$$(\mathbf{X}^\top \mathbf{X})^+ = \frac{|\mathbf{X}^\top \mathbf{X}| + \mathbf{X}^\top \mathbf{X}}{2}, \text{ and } (\mathbf{X}^\top \mathbf{X})^- = \frac{|\mathbf{X}^\top \mathbf{X}| - \mathbf{X}^\top \mathbf{X}}{2}. \quad (16)$$

The overall optimization method is summarized at Algorithm 1. Note that the constraints (i.e., $\mathbf{S} \geq 0$, $\mathbf{V} \geq 0$ and $\text{diag}(\mathbf{S}) = 0$) can be naturally satisfied by the above updating rules. See Section-IV for the detailed analysis.

Algorithm 1 Optimization method for Eq. (10)

Input: A predefined weight matrix \mathbf{W} , the data matrix \mathbf{X} , hyper-parameters α and β ;

Initialization: Assign \mathbf{S} and \mathbf{V} with positive random values;

- 1: **while** not converged **do**
 - 2: Update \mathbf{S} with fixed \mathbf{V} by Eq. (14);
 - 3: Update \mathbf{V} with fixed \mathbf{S} by Eq. (15);
 - 4: **end while**
 - 5: **Return** \mathbf{V} .
-

³As will be shown later in Section IV-A, this separation guarantees the non-negativity of \mathbf{S} and \mathbf{V} in the optimization procedure.

TABLE I
Datasets Description

Data set	# Samples (n)	# Classes (c)	# Dimensions (d)
Soybean	683	19	35
ECOIL	336	7	8
LIBRAS	360	15	90
YEAST	1484	10	8
IONSPHERE	351	2	34
BINALPHA	1404	36	320
IRIS	150	4	3
WINE	178	3	13
ISOLET	1560	26	617
MSRA	1799	12	256

C. Convergence Analysis of Algorithm 1

Theorem 1: Algorithm 1 has the following properties:

- 1) the objective value decreases (i.e., non-increases) at each iteration, and Algorithm 1 is locally convergent;
- 2) when convergent, the limiting point satisfies the KKT conditions, which indicates the correctness of it.
- 3) when both \mathbf{V} and \mathbf{S} are initialized with nonnegative matrices, the non-negativity for them are guaranteed at each iteration, i.e., $\mathbf{V}^t \geq 0$, $\mathbf{S}^t \geq 0$, $\forall t$. Moreover, when \mathbf{S} is initialized with a nonnegative matrix whose diagonal elements equal to zero, at each iteration, $\text{diag}(\mathbf{S}^t) = 0$, $\forall t$ is guaranteed.

See the detailed proof of Theorem 1 in the Appendix.

D. Computational Complexity

The sizes of \mathbf{X} , \mathbf{V} , \mathbf{S} , $\mathbf{X}^\top \mathbf{X}$ ⁴ are $d \times n$, $n \times c$, $n \times n$, $n \times n$, respectively. The computational complexities for $\mathbf{V}\mathbf{V}^\top$, $(\mathbf{X}^\top \mathbf{X})^- \mathbf{S}$, $(\mathbf{X}^\top \mathbf{X})^+ \mathbf{S}$, $\mathbf{S}\mathbf{V}$, $\mathbf{S}^\top \mathbf{V}$, $\mathbf{V}\mathbf{V}^\top \mathbf{V}$ are $O(n^2c)$, $O(n^3)$, $O(n^3)$, $O(n^2c)$, $O(n^2c)$, $O(2c^2n)$, respectively. Therefore, the computational complexity for step-2 and step-3 of Algorithm 1 are $O(n^2c + 2n^3)$ and $O(2n^2c + 2c^2n)$, respectively. And the overall complexity of each iteration of Algorithm 1 is $O(2n^3 + 3n^2c + 2c^2n)$. In addition, since Algorithm 2 has the similar computational steps as Algorithm 1, it has the same complexity as Algorithm 1.

IV. EXPERIMENTAL ANALYSIS

In this section, we conducted extensive experiments to validate the performance of the proposed model. Specifically, we compared the proposed model with 19 state-of-the-art methods on 10 commonly used datasets with 4 clustering metrics. Moreover, we adopted the Wilcoxon rank sum test [32] to assess whether the proposed model is significantly better or worse than the compared methods at a significance level of 0.05.

⁴Since $\mathbf{X}^\top \mathbf{X}$ can be computed in advance, it can be regarded as a single matrix in computing the complexity of each iteration.

A. Compared Models, Evaluation Metrics and Datasets

The evaluated methods are summarized as follows:

- 1, SymNMF [16], [15] is a low rank decomposition of graph matrix, which can directly produce the clustering result.
- 2, SC is a graph clustering method based on spectral decomposition. In this paper, we adopted the SC method presented in [13].
- 3, SSC [31] is convex formulation of SC that uses a sparse regularizer to pursue an ideal representation of the lower-dimensional embedding.
- 4, PCA is a linear dimensionality reduction method for data representation.
- 5, RPCA [33], [34] solves a convex optimization problem that is more robust to noise and outliers than the traditional PCA.
- 6, GLPCA [35] is a kind of PCA with a nonlinear graph regularization.
- 7, NMF [36] is a linear dimensionality reduction method that decomposes a nonnegative matrix into two nonnegative matrices with smaller sizes.
- 8, GNMF [37] is an NMF model with graph regularization.
- 9, GMF [38] is a graph regularized low rank matrix approximation method.
- 10, GRPCA [39] is a graph regularized robust PCA method.
- 11, K-means is a basic clustering method.
- 13, LRR [20], [40] is subspace clustering method with a low rank constraint on the coefficient matrix.
- 14, L2-Graph [22] is another subspace clustering method with a Frobenius norm on the coefficient matrix.
- 15, CAN [23] is a spectral clustering method with a learned graph according to the raw features.
- 16, RSS [41] simultaneously learns an affinity matrix and a subspace coefficient matrix. RSSA uses the affinity matrix to denote the graph weight matrix.
- 17, RSSR [41] uses the coefficient matrix to build the graph weight matrix.
- 18, RSSAR [41] adopts both the affinity matrix and coefficient matrix to construct the graph weight matrix.
- 19, To evaluate the effectiveness of the joint manner of graph construction and clustering, we made up a model termed L2-graph-SymNMF that first builds an L2-graph, then applies SymNMF on that graph to produce the clustering result.
- 20, ‘‘Proposed’’ denotes the proposed model.

For all the methods involving a graph structure, we adapted the same p NN graph, where p was empirically set to $\text{LR}(\log_2 n + 1)$ [18], σ equals to the mean distance of a sample to its p -nearest-neighbors, and $\text{LR}(x)$ returns the lower down round of x . Different methods have different hyper-parameters. For all the methods, the hyper-parameters were determined via exhaustive searching from $\{0.01, 0.1, 1, 10, 100, 1000\}$ for fair comparison. For all the graph learning methods like LLR and L2-graph, a standard SC [13] was adopted to produce the clustering result. For all the data representation methods like PCA and NMF and all the spectral clustering based methods like SC and SSC, K-means was performed on the embeddings

TABLE II
Clustering Performance on ECOIL

Methods	ACC	NMI	PUR	ARI
CAN	0.693 ↓	0.612 •	0.824 ↓	0.560 ↓
GLPCA	0.554 ± 0.067 ↓	0.529 ± 0.035 ↓	0.800 ± 0.021 ↓	0.422 ± 0.069 ↓
PCA	0.567 ± 0.061 ↓	0.402 ± 0.028 ↓	0.728 ± 0.016 ↓	0.346 ± 0.054 ↓
GMF	0.533 ± 0.055 ↓	0.513 ± 0.025 ↓	0.796 ± 0.027 ↓	0.389 ± 0.057 ↓
GNMF	<u>0.581 ± 0.056</u> ↓	0.473 ± 0.039 ↓	0.760 ± 0.030 ↓	<u>0.458 ± 0.093</u> ↓
GRPCA	0.651 ± 0.071 ↓	0.611 ± 0.043 •	<u>0.812 ± 0.022</u> ↓	0.554 ± 0.106 •
K-means	0.553 ± 0.067 ↓	<u>0.532 ± 0.032</u> ↓	0.804 ± 0.024 ↓	0.420 ± 0.024 ↓
L2-Graph	0.465 ± 0.032 ↓	0.334 ± 0.017 ↓	0.668 ± 0.019 ↓	0.220 ± 0.034 ↓
L2-SymNMF	0.502 ± 0.032 ↓	0.350 ± 0.015 ↓	0.665 ± 0.019 ↓	0.249 ± 0.0317 ↓
LRR	0.544 ± 0.071 ↓	0.524 ± 0.032 ↓	0.800 ± 0.022 ↓	0.414 ± 0.085 ↓
NMF	0.558 ± 0.054 ↓	0.446 ± 0.034 ↓	0.750 ± 0.026 ↓	0.417 ± 0.026 ↓
RPCA	0.547 ± 0.067 ↓	0.519 ± 0.024 ↓	<u>0.809 ± 0.019</u> ↓	0.405 ± 0.073 ↓
RSSAR	0.507 ± 0.034 ↓	0.431 ± 0.021 ↓	0.761 ± 0.019 ↓	0.315 ± 0.040 ↓
RSSR	0.486 ± 0.027 ↓	0.355 ± 0.015 ↓	0.708 ± 0.015 ↓	0.270 ± 0.021 ↓
RSSA	0.515 ± 0.025 ↓	0.429 ± 0.020 ↓	0.767 ± 0.018 ↓	0.331 ± 0.044 ↓
SC	0.544 ± 0.044 ↓	0.508 ± 0.029 ↓	0.818 ± 0.024 ↓	0.381 ± 0.024 ↓
SSC	<u>0.601 ± 0.036</u> ↓	0.492 ± 0.034 ↓	0.797 ± 0.037 ↓	0.357 ± 0.054 ↓
SymNMF	0.571 ± 0.070 ↓	0.506 ± 0.055 ↓	0.761 ± 0.056 ↓	0.401 ± 0.056 ↓
Proposed	0.735 ± 0.094	0.626 ± 0.046	0.836 ± 0.019	0.632 ± 0.130

to generate the final clustering result. To remove the influence of the randomness in K-means and initialization, we repeated each methods 20 times, and reported the mean values with standard deviation.

Clustering results were evaluated by the following commonly used metrics, i.e.,

- Clustering accuracy (ACC) first permutes the clustering partition according to the ground-truth label through a mapping function [42], then calculates the accuracy of the permuted labels.
- NMI is the normalized version of mutual information (MI), where MI measures correlation of two distributions. In clustering, the ground-truth labels and the clustering labels act as two distributions, where NMI computes how similar they are.
- Purity (PUR) first assigns each cluster to a class which is the most frequent in that cluster, then calculates the average accuracy of each cluster.
- Adjust rand index (ARI) computes how similar the clustering result and the ground truth labels are in a pairwise manner.

ACC, NMI and PUR all lay in the range of $[0, 1]$, while ARI lay in the range of $[-1, 1]$. Larger value indicates better clustering performance for all the metrics.

We selected 10 datasets to evaluate the performance of different methods. The number of samples varies from hundreds to thousands and the number of classes varies from 2 to 36. See the detailed information about those datasets from Table I.

B. Clustering Analysis

Tables II-XI show the clustering performance for different methods, and Tables XII-XIII summarize the overall performance of the proposed model on all the datasets. From those tables, we have the following observations and conclusions.

- 1) The proposed model always has higher clustering ACC/NMI/PUR/ARI than SymNMF over all the datasets. Especially, on IRIS, the ACC increases more

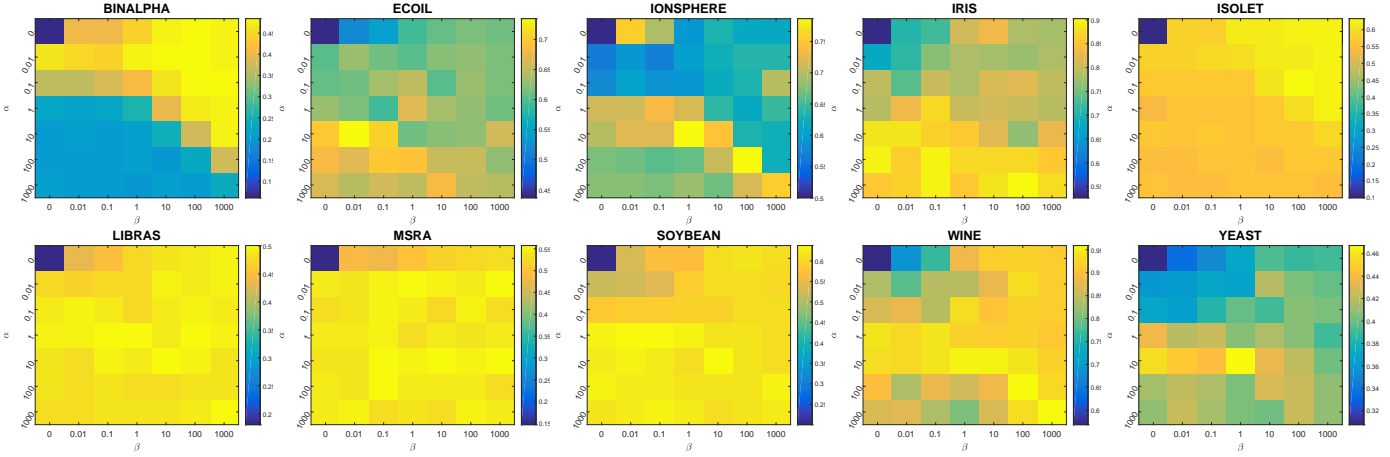


Fig. 1. Clustering ACC of the proposed model versus α and β on 10 datasets.

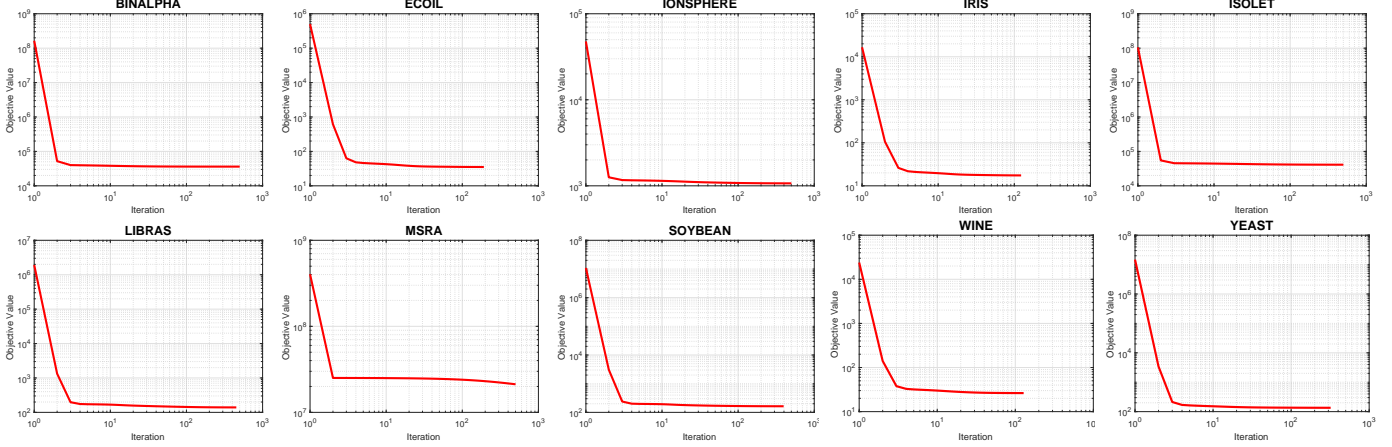


Fig. 2. Illustration of objective values against the number of iteration on 10 datasets.

TABLE III
Clustering Performance on YEAST

Methods	ACC	NMI	PUR	ARI
CAN	0.4218 ↓	0.1451 ↓	0.4299 ↓	0.0848 ↓
GLPCA	0.378 ± 0.024 ↓	0.248 ± 0.012 ↓	0.532 ± 0.011 ◇	0.148 ± 0.010 ↓
PCA	0.359 ± 0.019 ↓	0.233 ± 0.013 ↓	0.498 ± 0.023 ↓	0.134 ± 0.013 ↓
GMF	0.366 ± 0.025 ↓	0.239 ± 0.008 ↓	0.520 ± 0.006 ◇	0.138 ± 0.008 ↓
GNMF	0.323 ± 0.0322 ↓	0.190 ± 0.0294 ↓	0.466 ± 0.0211 ↓	0.101 ± 0.0266 ↓
GRPCA	0.451 ± 0.035 •	0.260 ± 0.031 •	0.535 ± 0.009 ◇	0.171 ± 0.031 •
K-means	0.378 ± 0.024 ↓	<u>0.249 ± 0.015</u> ↓	0.531 ± 0.013 ◇	0.148 ± 0.013 ↓
L2-Graph	0.358 ± 0.015 ↓	0.208 ± 0.007 ↓	0.502 ± 0.004 ↓	0.118 ± 0.008 ↓
L2-SymNMF	0.361 ± 0.021 ↓	0.222 ± 0.009 ↓	0.490 ± 0.013 ↓	0.123 ± 0.013 ↓
LRR	0.381 ± 0.022 ↓	0.251 ± 0.006 ↓	0.532 ± 0.010 ◇	<u>0.150 ± 0.007</u> ↓
NMF	0.334 ± 0.027 ↓	0.203 ± 0.024 ↓	0.484 ± 0.024 ↓	0.113 ± 0.024 ↓
RPCA	<u>0.384 ± 0.021</u> ↓	<u>0.249 ± 0.009</u> ↓	0.532 ± 0.013 ◇	<u>0.150 ± 0.009</u> ↓
RSSAR	0.331 ± 0.010 ↓	0.211 ± 0.007 ↓	0.510 ± 0.004 ↓	0.122 ± 0.006 ↓
RSSR	0.333 ± 0.016 ↓	0.208 ± 0.008 ↓	0.511 ± 0.004 ↓	0.118 ± 0.007 ↓
RSSA	0.327 ± 0.014 ↓	0.210 ± 0.004 ↓	0.512 ± 0.002 ↓	0.116 ± 0.004 ↓
SC	0.360 ± 0.011 ↓	0.245 ± 0.007 ↓	0.535 ± 0.008 ◇	<u>0.151 ± 0.008</u> ↓
SSC	0.383 ± 0.021 ↓	<u>0.249 ± 0.012</u> ↓	0.527 ± 0.010 •	0.149 ± 0.010 ↓
SymNMF	0.404 ± 0.045 ↓	0.208 ± 0.040 ↓	0.426 ± 0.037 ↓	0.152 ± 0.037 ↓
Proposed	0.467 ± 0.048	0.273 ± 0.021	0.518 ± 0.019	0.186 ± 0.048

than 35% compared with SymNMF. Moreover, according to the Wilcoxon rank sum test, the improvements under all the cases (40/40) are significant, which validates our basic assumption that a predefined similarity

TABLE IV
Clustering Performance on IONSPHERE

Methods	ACC	NMI	PUR	ARI
CAN	0.547 ↓	0.054 ↓	0.641 ↓	-0.0455 ↓
GLPCA	0.658 ± 0.001 ↓	0.139 ± 0.074 ↓	0.675 ± 0.026 ↓	0.095 ± 0.001 ↓
PCA	0.514 ± 0.0035 ↓	0.021 ± 0.0051 ↓	0.641 ± 0 ↓	-0.026 ± 0.0018 ↓
GMF	0.704 ± 0.024 ↓	0.104 ± 0.007 ↓	0.704 ± 0.024 ↓	0.135 ± 0 ↓
GNMF	—	—	—	—
GRPCA	0.727 ± 0.032 ↓	<u>0.149 ± 0.056</u> ↓	0.727 ± 0.032 ↓	0.177 ± 0 ↓
K-means	0.708 ± 0.015 ↓	0.124 ± 0.028 ↓	0.708 ± 0.015 ↓	0.167 ± 0.015 ↓
L2-Graph	0.555 ± 0 ↓	0.153 ± 0 ↓	0.641 ± 0 ↓	-0.017 ± 0.002 ↓
L2-SymNMF	0.671 ± 0.106 ↓	0.199 ± 0.109 •	0.706 ± 0.061 ↓	0.145 ± 0.146 ↓
LRR	<u>0.711 ± 0.001</u> ↓	0.130 ± 0.001 ↓	<u>0.711 ± 0.001</u> ↓	<u>0.176 ± 0.002</u> ↓
NMF	—	—	—	—
RPCA	<u>0.711 ± 0.001</u> ↓	0.130 ± 0.001 ↓	<u>0.711 ± 0.001</u> ↓	<u>0.176 ± 0.002</u> ↓
RSSRA	0.529 ± 0 ↓	0.131 ± 0 ↓	0.641 ± 0 ↓	-0.0336 ± 0 ↓
RSSR	0.555 ± 0 ↓	0.117 ± 0 ↓	0.641 ± 0 ↓	-0.016 ± 0 ↓
RSSA	0.529 ± 0 ↓	0.131 ± 0 ↓	0.641 ± 0 ↓	-0.033 ± 0 ↓
SC	0.643 ± 0 ↓	0.046 ± 0 ↓	0.643 ± 0 ↓	0.077 ± 0 ↓
SSC	0.766 ± 0 ↓	0.205 ± 0 ↓	0.766 ± 0 ↓	0.281 ± 0 ↓
SymNMF	0.652 ± 0.080 ↓	0.111 ± 0.071 ↓	0.679 ± 0.051 ↓	0.110 ± 0.051 ↓
Proposed	0.787 ± 0.066	0.256 ± 0.065	0.790 ± 0.056	0.339 ± 0.123

graph is usually not the best choice. By learning a reasonable graph from raw features, the proposed model can generate a higher quality graph.

2) Since NMF and GNMF require the input data to be

TABLE V
Clustering Performance on BINALPHA

Methods	ACC	NMI	PUR	ARI
CAN	0.332 ↓	0.445 ↓	0.363 ↓	0.091 ↓
GLPCA	0.409 ± 0.022 ↓	0.570 ± 0.010 ↓	0.439 ± 0.018 ↓	0.268 ± 0.015 ↓
PCA	0.352 ± 0.022 ↓	0.512 ± 0.015 ↓	0.376 ± 0.021 ↓	0.210 ± 0.017 ↓
GMF	0.449 ± 0.016 ↓	0.606 ± 0.008 ↓	0.487 ± 0.015 ↓	0.307 ± 0.013 ↓
GNMF	0.366 ± 0.018 ↓	0.523 ± 0.013 ↓	0.392 ± 0.017 ↓	0.218 ± 0.014 ↓
GRPCA	0.458 ± 0.020 ↓	0.619 ± 0.009●	0.490 ± 0.017 ↓	0.328 ± 0.012 ↓
K-means	0.394 ± 0.015 ↓	0.564 ± 0.010 ↓	0.425 ± 0.016 ↓	0.259 ± 0.016 ↓
L2-Graph	0.345 ± 0.010 ↓	0.481 ± 0.007 ↓	0.374 ± 0.009 ↓	0.192 ± 0.008 ↓
L2-SymNMF	0.312 ± 0.013 ↓	0.452 ± 0.008 ↓	0.352 ± 0.012 ↓	0.172 ± 0.009 ↓
LLR	0.414 ± 0.025 ↓	0.573 ± 0.010 ↓	0.443 ± 0.022 ↓	0.272 ± 0.015 ↓
NMF	0.357 ± 0.017 ↓	0.518 ± 0.013 ↓	0.386 ± 0.017 ↓	0.211 ± 0.017 ↓
RPCA	0.412 ± 0.017 ↓	0.572 ± 0.008 ↓	0.442 ± 0.014 ↓	0.273 ± 0.016 ↓
RSSAR	0.121 ± 0.004 ↓	0.185 ± 0.006 ↓	0.131 ± 0.003 ↓	0.023 ± 0.004 ↓
RSSR	0.203 ± 0.011 ↓	0.309 ± 0.006 ↓	0.216 ± 0.010 ↓	0.075 ± 0.005 ↓
RSSA	0.116 ± 0.003 ↓	0.185 ± 0.007 ↓	0.124 ± 0.003 ↓	0.014 ± 0.002 ↓
SC	0.477 ± 0.018●	0.615 ± 0.008 ↓	0.506 ± 0.014 ↓	0.329 ± 0.014 ↓
SSC	0.466 ± 0.020 ↓	0.613 ± 0.010 ↓	0.501 ± 0.018 ↓	0.327 ± 0.016 ↓
SymNMF	0.465 ± 0.019 ↓	0.619 ± 0.009●	0.504 ± 0.016 ↓	0.335 ± 0.016●
Proposed	0.484 ± 0.018	0.622 ± 0.010	0.516 ± 0.017	0.337 ± 0.015

TABLE VI
Clustering Performance on IRIS

Methods	ACC	NMI	PUR	ARI
CAN	0.693 ↓	0.596 ↓	0.693 ↓	0.560 ↓
GLPCA	0.520 ± 0.083 ↓	0.228 ± 0.014 ↓	0.556 ± 0.042 ↓	0.148 ± 0.137 ↓
PCA	0.722 ± 0.121 ↓	0.597 ± 0.011 ↓	0.760 ± 0.062 ↓	0.528 ± 0.053 ↓
GMF	0.821 ± 0.141 ↓	0.704 ± 0.089 ↓	0.845 ± 0.091 ↓	0.663 ± 0.125 ↓
GNMF	0.776 ± 0.067 ↓	0.626 ± 0.034 ↓	0.780 ± 0.057 ↓	0.567 ± 0.053 ↓
GRPCA	0.884 ± 0.085●	0.781 ± 0.047●	0.892 ± 0.053●	0.737 ± 0.070●
K-means	0.757 ± 0.183 ↓	0.668 ± 0.101 ↓	0.811 ± 0.108 ↓	0.615 ± 0.108 ↓
L2 Graph	0.830 ± 0.019 ↓	0.663 ± 0.015 ↓	0.830 ± 0.019 ↓	0.621 ± 0.022 ↓
L2-SymNMF	0.807 ± 0.006 ↓	0.638 ± 0.026 ↓	0.807 ± 0.006 ↓	0.585 ± 0.009 ↓
LRR	0.852 ± 0.115 ↓	0.722 ± 0.065 ↓	0.867 ± 0.068 ↓	0.693 ± 0.093 ↓
NMF	0.719 ± 0.112 ↓	0.614 ± 0.098 ↓	0.738 ± 0.087 ↓	0.545 ± 0.087 ↓
RPCA	0.838 ± 0.125 ↓	0.711 ± 0.077 ↓	0.856 ± 0.081 ↓	0.677 ± 0.109 ↓
RSSAR	0.510 ± 0.026 ↓	0.419 ± 0.069 ↓	0.615 ± 0.022 ↓	0.312 ± 0.065 ↓
RSSR	0.826 ± 0 ↓	0.652 ± 0.001 ↓	0.826 ± 0 ↓	0.610 ± 0.001 ↓
RSSA	0.519 ± 0.029 ↓	0.579 ± 0 ↓	0.666 ± 0 ↓	0.442 ± 0.009 ↓
SC	0.461 ± 0.002 ↓	0.298 ± 0.004 ↓	0.561 ± 0.002 ↓	0.187 ± 0.002 ↓
SSC	0.854 ± 0.115 ↓	0.725 ± 0.066 ↓	0.869 ± 0.069 ↓	0.695 ± 0.094 ↓
SymNMF	0.665 ± 0.126 ↓	0.417 ± 0.170 ↓	0.681 ± 0.116 ↓	0.384 ± 0.116 ↓
Proposed	0.903 ± 0.005	0.786 ± 0.012	0.903 ± 0.005	0.751 ± 0.011

TABLE VII
Clustering Performance on WINE

Methods	ACC	NMI	PUR	ARI
CAN	0.668 ↓	0.521 ↓	0.707 ↓	0.490 ↓
GLPCA	0.923 ± 0.005 ↓	0.767 ± 0.012 ↓	0.923 ± 0.005 ↓	0.773 ± 0.015 ↓
PCA	0.929 ± 0.002 ↓	0.764 ± 0.006 ↓	0.929 ± 0.002 ↓	0.789 ± 0.007 ↓
GMF	0.921 ± 0 ↓	0.754 ± 0 ↓	0.921 ± 0 ↓	0.768 ± 0 ↓
GNMF	0.918 ± 0.009 ↓	0.741 ± 0.025 ↓	0.918 ± 0.009 ↓	0.761 ± 0.025 ↓
GRPCA	0.923 ± 0.005 ↓	0.776 ± 0.004 ↓	0.923 ± 0.005 ↓	0.774 ± 0.014 ↓
K-means	0.923 ± 0.005 ↓	0.766 ± 0.011 ↓	0.923 ± 0.005 ↓	0.773 ± 0.005 ↓
L2-Graph	0.946 ± 0.002 ↓	0.808 ± 0.009 ↓	0.946 ± 0.002 ↓	0.837 ± 0.008 ↓
L2-SymNMF	0.874 ± 0.134 ↓	0.713 ± 0.155 ↓	0.881 ± 0.117 ↓	0.722 ± 0.183 ↓
LRR	0.924 ± 0.004 ↓	0.769 ± 0.009 ↓	0.924 ± 0.004 ↓	0.776 ± 0.012 ↓
NMF	0.854 ± 0.107 ↓	0.654 ± 0.129 ↓	0.857 ± 0.099 ↓	0.648 ± 0.099 ↓
RPCA	0.926 ± 0.008 ↓	0.779 ± 0.024 ↓	0.926 ± 0.008 ↓	0.782 ± 0.022 ↓
RSSAR	0.927 ± 0.088 ↓	0.797 ± 0.075 ↓	0.930 ± 0.073 ↓	0.817 ± 0.103 ↓
RSSR	0.935 ± 0.002 ↓	0.801 ± 0.006 ↓	0.935 ± 0.002 ↓	0.809 ± 0.007 ↓
RSSA	0.921 ± 0 ↓	0.741 ± 0 ↓	0.921 ± 0 ↓	0.770 ± 0 ↓
SC	0.949 ± 0 ↓	0.829 ± 0 ↓	0.949 ± 0 ↓	0.848 ± 0 ↓
SSC	0.903 ± 0.088 ↓	0.766 ± 0.086 ↓	0.909 ± 0.070 ↓	0.765 ± 0.105 ↓
SymNMF	0.852 ± 0.128 ↓	0.667 ± 0.147 ↓	0.856 ± 0.116 ↓	0.667 ± 0.116 ↓
Proposed	0.959 ± 0.004	0.852 ± 0.109	0.959 ± 0.004	0.881 ± 0.127

TABLE VIII
Clustering Performance on MSRA

Methods	ACC	NMI	PUR	ARI
CAN	0.533 ↓	0.602 ↓	0.537 ↓	0.313 ↓
GLPCA	0.514 ± 0.033 ↓	0.583 ± 0.032 ↓	0.541 ± 0.030 ↓	0.349 ± 0.045 ↓
PCA	0.525 ± 0.030 ↓	0.585 ± 0.029 ↓	0.551 ± 0.027 ↓	0.378 ± 0.041 ↓
GMF	0.495 ± 0.037 ↓	0.553 ± 0.031 ↓	0.522 ± 0.029 ↓	0.324 ± 0.043 ↓
GNMF	0.497 ± 0.034 ↓	0.559 ± 0.032 ↓	0.525 ± 0.029 ↓	0.345 ± 0.036 ↓
GRPCA	0.546 ± 0.049●	0.667 ± 0.034●	0.584 ± 0.041●	0.409 ± 0.044●
K-means	0.497 ± 0.040 ↓	0.573 ± 0.033 ↓	0.529 ± 0.033 ↓	0.342 ± 0.033 ↓
L2-Graph	0.539 ± 0.037●	0.646 ± 0.048 ↓	0.587 ± 0.033●	0.369 ± 0.059 ↓
L2-SymNMF	0.566 ± 0.039●	0.688 ± 0.026◇	0.610 ± 0.031◇	0.463 ± 0.043◇
LRR	0.512 ± 0.034 ↓	0.594 ± 0.031 ↓	0.548 ± 0.027 ↓	0.364 ± 0.041 ↓
NMF	0.484 ± 0.035 ↓	0.539 ± 0.031 ↓	0.507 ± 0.029 ↓	0.321 ± 0.029 ↓
RPCA	0.520 ± 0.036 ↓	0.589 ± 0.029 ↓	0.547 ± 0.027 ↓	0.359 ± 0.032 ↓
RSSAR	0.549 ± 0.041●	0.565 ± 0.020 ↓	0.593 ± 0.031●	0.335 ± 0.042 ↓
RSSR	0.642 ± 0.029◇	0.736 ± 0.027◇	0.690 ± 0.029◇	0.548 ± 0.038◇
RSSA	0.509 ± 0.020 ↓	0.485 ± 0.013 ↓	0.542 ± 0.020 ↓	0.275 ± 0.021 ↓
SC	0.447 ± 0.027 ↓	0.546 ± 0.022 ↓	0.484 ± 0.025 ↓	0.292 ± 0.025 ↓
SSC	0.495 ± 0.046 ↓	0.566 ± 0.039 ↓	0.532 ± 0.042 ↓	0.335 ± 0.049 ↓
SymNMF	0.457 ± 0.027 ↓	0.569 ± 0.027 ↓	0.502 ± 0.029 ↓	0.333 ± 0.029 ↓
Proposed	0.557 ± 0.045	0.673 ± 0.032	0.588 ± 0.038	0.432 ± 0.041

TABLE IX
Clustering Performance on ISOLET

Methods	ACC	NMI	PUR	ARI
CAN	0.553 ↓	0.733 ↓	0.590 ↓	0.416 ↓
GLPCA	0.589 ± 0.037 ↓	0.744 ± 0.016 ↓	0.632 ± 0.028 ↓	0.528 ± 0.033 ↓
PCA	0.635 ± 0.047●	0.750 ± 0.024 ↓	0.675 ± 0.040●	0.563 ± 0.035●
GNMF	—	—	—	—
GRPCA	0.593 ± 0.034 ↓	0.752 ± 0.011 ↓	0.633 ± 0.020 ↓	0.540 ± 0.018 ↓
K-means	0.588 ± 0.034 ↓	0.742 ± 0.019 ↓	0.631 ± 0.031 ↓	0.524 ± 0.031 ↓
L2-Graph	0.547 ± 0.036 ↓	0.702 ± 0.016 ↓	0.587 ± 0.026 ↓	0.472 ± 0.033 ↓
L2-SymNMF	0.523 ± 0.019 ↓	0.682 ± 0.014 ↓	0.585 ± 0.018 ↓	0.443 ± 0.024 ↓
LRR	0.601 ± 0.024 ↓	0.749 ± 0.013 ↓	0.639 ± 0.023 ↓	0.536 ± 0.021 ↓
NMF	—	—	—	—
RPCA	0.593 ± 0.026 ↓	0.745 ± 0.012 ↓	0.632 ± 0.024 ↓	0.529 ± 0.027 ↓
RSSAR	0.217 ± 0.006 ↓	0.266 ± 0.004 ↓	0.245 ± 0.004 ↓	0.074 ± 0.003 ↓
RSSR	0.366 ± 0.018 ↓	0.476 ± 0.010 ↓	0.397 ± 0.015 ↓	0.243 ± 0.010 ↓
RSSA	0.221 ± 0.009 ↓	0.224 ± 0.004 ↓	0.254 ± 0.008 ↓	0.072 ± 0.003 ↓
SC	0.583 ± 0.037 ↓	0.743 ± 0.014 ↓	0.620 ± 0.029 ↓	0.512 ± 0.029 ↓
SSC	0.547 ± 0.037 ↓	0.720 ± 0.019 ↓	0.583 ± 0.027 ↓	0.477 ± 0.034 ↓
SymNMF	0.582 ± 0.023 ↓	0.774 ± 0.010 ↓	0.659 ± 0.017 ↓	0.536 ± 0.017 ↓
Proposed	0.633 ± 0.024	0.781 ± 0.005	0.685 ± 0.014	0.571 ± 0.013

TABLE X
Clustering Performance on LIBRAS

Methods	ACC	NMI	PUR	ARI
CAN	0.483 ↓	0.654◇	0.525 ↓	0.398●
GLPCA	0.442 ± 0.019 ↓	0.572 ± 0.017 ↓	0.469 ± 0.024 ↓	0.303 ± 0.019 ↓
PCA	0.431 ± 0.022 ↓	0.506 ± 0.018 ↓	0.459 ± 0.019 ↓	0.237 ± 0.020 ↓
GMF	0.445 ± 0.030 ↓	0.577 ± 0.020 ↓	0.479 ± 0.029 ↓	0.303 ± 0.022 ↓
GNMF	0.463 ± 0.028 ↓	0.564 ± 0.030 ↓	0.490 ± 0.023 ↓	0.300 ± 0.034 ↓
GRPCA	0.464 ± 0.033 ↓	0.593 ± 0.027 ↓	0.494 ± 0.027 ↓	0.236 ± 0.031 ↓
K-means	0.435 ± 0.023 ↓	0.562 ± 0.023 ↓	0.464 ± 0.025 ↓	0.293 ± 0.025 ↓
L2-graph	0.497 ± 0.028●	0.622 ± 0.026 ↓	0.524 ± 0.021●	0.361 ± 0.018 ↓
L2-SymNMF	0.521 ± 0.022◇	0.639 ± 0.018●	0.544 ± 0.016◇	0.383 ± 0.024 ↓
LRR	0.440 ± 0.023 ↓	0.569 ± 0.015 ↓	0.469 ± 0.021 ↓	0.299 ± 0.018 ↓
NMF	0.460 ± 0.032 ↓	0.558 ± 0.024 ↓	0.493 ± 0.025 ↓	0.296 ± 0.025 ↓
RPCA	0.444 ± 0.027 ↓	0.569 ± 0.020 ↓	0.470 ± 0.022 ↓	0.300 ± 0.022 ↓
RSSAR	0.492 ± 0.024●	0.604 ± 0.020 ↓	0.519 ± 0.024●	0.340 ± 0.022 ↓
RSSR	0.476 ± 0.027 ↓	0.574 ± 0.016 ↓	0.506 ± 0.023 ↓	0.314 ± 0.022 ↓
RSSA	0.472 ± 0.024 ↓	0.594 ± 0.015 ↓	0.496 ± 0.016 ↓	0.331 ± 0.020 ↓
SC	0.466 ± 0.030 ↓	0.615 ± 0.023 ↓	0.500 ± 0.025 ↓	0.347 ± 0.025 ↓
SSC	0.457 ± 0.032 ↓	0.600 ± 0.022 ↓	0.495 ± 0.023 ↓	0.336 ± 0.033 ↓
SymNMF	0.482 ± 0.023 ↓	0.619 ± 0.020 ↓	0.520 ± 0.019 ↓	0.356 ± 0.020 ↓
Proposed	0.501 ± 0.023	0.643 ± 0.012	0.532 ± 0.011	0.397 ± 0.016

nonnegative, and IONSHPERE and ISOLET are consisted of mixed signed data, NMF and GNMF are not

applicable to IONSHPERE and ISOLET. Although our model also contains the nonnegative constraints on \mathbf{S} and \mathbf{V} , it can cope with the mixed sign data by separating

TABLE XI
Clustering Performance on SOYBEAN

Methods	ACC	NMI	PUR	ARI
CAN	0.540 ↓	0.697 ↓	0.638 ↓	0.341 ↓
GLPCA	0.573 ± 0.029 ↓	0.700 ± 0.021 ↓	0.675 ± 0.030 ↓	0.445 ± 0.044 ●
PCA	0.591 ± 0.035 ↓	0.688 ± 0.022 ↓	0.690 ± 0.029 ↓	0.446 ± 0.048 ●
GMF	0.551 ± 0.049 ↓	0.689 ± 0.033 ↓	0.667 ± 0.040 ↓	0.420 ± 0.057 ●
GNMF	0.605 ± 0.039 ↓	0.715 ± 0.021 ↓	0.704 ± 0.026 ●	0.475 ± 0.045 ◇
GRPCA	0.576 ± 0.043 ↓	0.710 ± 0.027 ↓	0.676 ± 0.027 ↓	0.445 ± 0.050 ●
K-means	0.560 ± 0.033 ↓	0.699 ± 0.022 ↓	0.659 ± 0.037 ↓	0.424 ± 0.037 ●
L2-Graph	0.588 ± 0.026 ↓	0.730 ± 0.018 ↓	0.692 ± 0.026 ●	0.424 ± 0.025 ●
L2-SymNMF	0.593 ± 0.042 ↓	0.728 ± 0.027 ↓	0.697 ± 0.031 ●	0.422 ± 0.045 ●
LRR	0.566 ± 0.039 ↓	0.698 ± 0.027 ↓	0.666 ± 0.032 ↓	0.439 ± 0.057 ●
NMF	0.598 ± 0.043 ↓	0.718 ± 0.021 ↓	0.709 ± 0.031 ●	0.461 ± 0.031 ◇
RPCA	0.570 ± 0.030 ↓	0.700 ± 0.015 ↓	0.668 ± 0.024	0.435 ± 0.041 ●
RSSAR	0.573 ± 0.041 ↓	0.715 ± 0.028 ↓	0.693 ± 0.030 ↓	0.442 ± 0.037 ●
RSSR	0.578 ± 0.053 ↓	0.703 ± 0.014 ↓	0.696 ± 0.037 ●	0.442 ± 0.034 ●
RSSA	0.558 ± 0.043 ↓	0.700 ± 0.024 ↓	0.671 ± 0.038 ↓	0.414 ± 0.034 ●
SC	0.495 ± 0.038 ↓	0.641 ± 0.026 ↓	0.604 ± 0.040 ↓	0.355 ± 0.040 ↓
SSC	0.574 ± 0.031 ↓	0.704 ± 0.020 ↓	0.672 ± 0.031 ↓	0.441 ± 0.038 ●
SymNMF	0.513 ± 0.042 ↓	0.664 ± 0.020 ↓	0.0620 ± 0.029 ↓	0.326 ± 0.029 ↓
Proposed	0.638 ± 0.025	0.744 ± 0.017	0.713 ± 0.025	0.428 ± 0.050

TABLE XII
Rank Counting for the Proposed Method

	Rank 1	Rank 2~3	Rank 4~5	Rank 6~20
Quantity	29/40	8/40	1/40	2/40
Ratio	72.5%	20.0%	2.5%	5%

TABLE XIII
Is the Proposed Model Significantly Better than Others

	Significantly better	No significant difference	Significantly worse
Quantity	634/704	51/704	19/704
Ratio	90.1%	7.2%	2.7%

the negative and positive components in $\mathbf{X}^T \mathbf{X}$, which is more flexible than NMF-like methods.

- SymNMF usually performs better than SC on the majority cases (29/40). Taking IRIS as an example, ACC increases 45% and PUR increases 105%. Note that both SymNMF and SC utilize the same predefined similarity graph matrix in the experiments, the advantage of SymNMF over SC validates that directly generating data partition is beneficial to clustering, which is also adopted in our model.
- CAN is a graph clustering method with an adaptive graph according to the raw features that performs well on some datasets, and SSC is an advanced SC method based on the predefined graph. CAN performs better than SSC on ECOIL, LIBRAS, YEAST and MSRA, while SSC performs better than CAN on IONSPHERE, ISOLET, SOYBEAN, BINALPHA, WINE and IRIS. This phenomenon demonstrates that both the raw features and the predefined graph are important to clustering if they are well exploited.
- Real world data are always full of different kinds of noises and outliers, therefore models that robust to noises and outliers may produce high quality clustering result. For example, robust models like RPCA and

GRPCA get quite well performance on ECOIL, YEAST, IONSPHERE, IRIS, BINAPHPA and ISOLET. Moreover, according to the IPD property of L2 norm [22], the L2-graph is also robust to noise, which is also applicable to our model.

- The methods with a graph regularizer usually perform better than the original models. For example, GNMF performs better than NMF and GMF performs better than PCA. This phenomenon exposes the importance of local structures in clustering. Both PCA and NMF can be regarded as variants of K-means [43], [44] in a soft manner, and the graph regularizer is highly related to spectral clustering [45]. These phenomena also suggest that graph clustering can usually generate better partition than K-means like methods.
- The proposed model performs significantly better than L2-graph on the majority cases (34/40) according to the Wilcoxon rank-sum test. It also obtains higher performance than L2-SymNMF over the majority cases (34/40). Especially, (30/40) of them are significantly better. Taking ECOIL as an example, the proposed model generates approximate 50% higher ACC than L2-graph and L2-SymNMF. Both L2 graph L2-SymNMF learn graph from the raw features with a Frobenius norm on the coefficient matrix like our model. While our method is processed in a joint manner with clustering. Those phenomena verify the benefit of the proposed joint manner.
- Table XII summarizes the ranking of the proposed model among all the 20 methods on all the datasets with different metrics. What is noteworthy in Table XII is that the proposed model obtains the highest rank under 29 out of 40 cases (72.5%). Moreover, the proposed model rank top 3 under (92.5%) cases. Table XIII sums up whether the proposed method is significantly better, or worse than the compared methods. It is apparent from Table XIII that the proposed model performs significantly better than the compared methods under more than 90% cases and only under less than 3% cases that the proposed model gets significantly worse results. Above analyses support the conclusion that the proposed model produce better clustering performance than the compared 19 models on those 10 datasets.

C. Parameter Sensitiveness

There are two hyper-parameters in the proposed model, where α and β adjust the contributions from the raw features and the predefined graph, respectively, to graph construction. Fig. 1 plots the values of ACC w.r.t. different α and β , where we can see that

- The highest ACC never occurs when $\alpha = 0$ or $\beta = 0$, which indicates that both α and β are critical to the proposed model. Moreover, the lowest value always appear when both $\alpha = 0$ and $\beta = 0$. The reason is straightforward, when $\alpha = \beta = 0$, no useful information can be transferred to the clustering membership matrix \mathbf{V} .

- 2) The optimal ACCs of all the datasets usually occur on a common range, i.e., $\alpha \in \{0.1, 10\}$, and $\beta \in \{1, 100\}$, which validate the robustness of our model to hyper-parameters.

D. Convergence Analysis

The convergence of the proposed optimization method has been theoretical shown in section IV. In this section we study the empirical convergence behavior of the proposed optimization method. Fig. 2 plots objective values against the increasing of iteration numbers with $\alpha = 1$ and $\beta = 1$ on all the datasets. From Fig. 2 we can see that the objective values decrease monotonically on all the datasets with the increasing of iteration, which is consistent with the theoretical analysis. Moreover, on all the datasets the objective values get convergent in approximate 100 iterations, which illustrates the high efficiency of our optimization method.

V. CONCLUSION

In this paper, we have presented a graph clustering model by directly producing data partition and learning a graph matrix in a joint manner, which exploits the mutual enhancement relation between them. The graph matrix is adaptively constructed by collecting the information from the original graph, the raw features and the clustering membership matrix. In addition, the proposed model is solved via an alternative optimization method, which can converge to the KKT points under some mild conditions. Extensive experiments indicate that the proposed model has higher clustering performance than 19 compared state-of-the-art methods significantly according to the Wilcoxon rank-sum test.

The proposed model explores the information from raw features in a linear manner, i.e., $\min_{\mathbf{S}} \|\mathbf{X} - \mathbf{X}\mathbf{S}\|_F^2$. Since Eq. (15) only relates to the inner product of input (i.e., $\mathbf{X}^T\mathbf{X}$), the proposed model has potential for exploiting the non-linear relation in raw features with a kernel trick.

APPENDIX A PROOF OF THEOREM 1

A. Proof of Theorem 1-1

According to [36], the following Lemma and Definition can be used to prove Theorem 1-1.

Definition 1 $g(h, h')$ is a upper-bound auxiliary function for $f(h)$ if the following two conditions are satisfied

$$g(h, h') \geq f(h), \text{ and, } g(h, h) = f(h). \quad (17)$$

Lemma 1 If g is a upper-bound auxiliary function of f , f is non-increasing under the update

$$h = \operatorname{argmin}_h g(h, h'). \quad (18)$$

See the proof of Lemma 1 at [36]. Based on Lemma 1, if we can find appropriate upper-bound auxiliary functions for Eq. (10) w.r.t. \mathbf{S} and \mathbf{V} , respectively, and then show the updating rules in Eq. (14) and Eq. (15) decrease the corresponding upper-bound functions, Theorem 1-1 can be proved.

Excluding terms uncorrelated to \mathbf{S} , the objective function for \mathbf{S} is written as

$$\begin{aligned} \mathcal{O}_{\mathbf{S}} = & \operatorname{Tr} \left((1 + \beta) \mathbf{S} \mathbf{S}^T + \alpha \mathbf{S} \mathbf{S}^T \mathbf{X}^T \mathbf{X} - 2\alpha \mathbf{X}^T \mathbf{X} \mathbf{S}^T \right. \\ & \left. - 2 \left(\mathbf{V} \mathbf{V}^T + \beta \mathbf{W} \right) \mathbf{S}^T \right) + \text{const.} \\ & \propto \operatorname{Tr} \left(\mathbf{S}^T \mathbf{A} \mathbf{S} - \mathbf{S}^T \mathbf{B} \mathbf{S} - \mathbf{S}^T \mathbf{C} + \mathbf{S}^T \mathbf{D} \right) \end{aligned} \quad (19)$$

where $\mathbf{A} = (1 + \beta) \mathbf{I} + \alpha (\mathbf{X}^T \mathbf{X})^+$, $\mathbf{B} = \alpha (\mathbf{X}^T \mathbf{X})^-$, $\mathbf{C} = 2\mathbf{V} \mathbf{V}^T + 2\beta \mathbf{W} + 2\alpha (\mathbf{X}^T \mathbf{X})^+$, and $\mathbf{D} = 2\mathbf{B} = 2\alpha (\mathbf{X}^T \mathbf{X})^-$.

For the \mathbf{V} -block, its corresponding objective function is

$$\begin{aligned} \mathcal{O}_{\mathbf{V}} = & \operatorname{Tr} \left(-2\mathbf{V} \mathbf{V}^T \mathbf{S}^T + \mathbf{V} \mathbf{V}^T \mathbf{V} \mathbf{V}^T \right) + \text{const} \\ & \propto \operatorname{Tr} \left(-2\mathbf{V} \mathbf{V}^T \mathbf{S}^T + \mathbf{V} \mathbf{V}^T \mathbf{V} \mathbf{V}^T \right). \end{aligned} \quad (20)$$

The adopted upper-bound auxiliary for Eqs. (19) and (20) are given in the following two lemmas.

Lemma 2 The upper bound auxiliary function for Eq. (19) is

$$\begin{aligned} f_s(\mathbf{S}, \mathbf{S}') = & - \sum_{ijk} \mathbf{B}_{ik} \mathbf{S}'_{ki} \mathbf{S}'_{ij} \left(1 + \log \frac{\mathbf{S}_{ki} \mathbf{S}_{ij}}{\mathbf{S}'_{ki} \mathbf{S}'_{ij}} \right) \\ & + \sum_{i,j} \frac{(\mathbf{A} \mathbf{S}')_{i,j} \mathbf{S}_{i,j}^2}{\mathbf{S}'_{i,j}} + \sum_{i,j} \mathbf{D}_{i,j} \frac{\mathbf{S}_{i,j}^2 + \mathbf{S}'_{i,j}^2}{2\mathbf{S}'_{i,j}} \\ & - \sum_{i,j} \mathbf{C}_{i,j} \mathbf{S}'_{i,j} \left(1 + \log \frac{\mathbf{S}_{i,j}}{\mathbf{S}'_{i,j}} \right). \end{aligned} \quad (21)$$

Lemma 3 The upper-bound auxiliary function for Eq. (20) is

$$\begin{aligned} f_v(\mathbf{V}, \mathbf{V}') = & \sum_{i,j}^n \sum_{k=1}^c (\mathbf{V}' \mathbf{V}'^T)_{i,j} \mathbf{V}'_{ik} \times \frac{\mathbf{V}_{jk}^4}{\mathbf{V}'_{jk}^3} \\ & - 2 \sum_{i,j}^n \sum_{k=1}^c \mathbf{S}_{ji} \mathbf{V}'_{jk} \mathbf{V}'_{ik} \left(1 + \log \frac{\mathbf{V}_{jk} \mathbf{V}_{ik}}{\mathbf{V}'_{jk} \mathbf{V}'_{ik}} \right). \end{aligned} \quad (22)$$

Proof of Lemma 2: Lemma 2 can be proved based on the following 4 inequalities.

Proposition 1 For any positive matrices $\mathbf{A} > 0$, $\mathbf{B} > 0$, $\mathbf{C} > 0$, $\mathbf{D} > 0$, $\mathbf{S} > 0$ and $\mathbf{S}' > 0$, with \mathbf{A} symmetric, the following equations hold:

$$\operatorname{tr}(\mathbf{S}^T \mathbf{A} \mathbf{S}) \leq \sum_{i,j} \frac{(\mathbf{A} \mathbf{S}')_{i,j} \mathbf{S}_{i,j}^2}{\mathbf{S}'_{i,j}}, \quad (23a)$$

$$\operatorname{tr}(\mathbf{S}^T \mathbf{B} \mathbf{S}) \geq \sum_{ijk} \mathbf{B}_{jk} \mathbf{S}'_{ki} \mathbf{S}'_{ji} \left(1 + \log \frac{\mathbf{S}_{ki} \mathbf{S}_{ji}}{\mathbf{S}'_{ki} \mathbf{S}'_{ji}} \right), \quad (23b)$$

$$\operatorname{tr}(\mathbf{S}^T \mathbf{C}) \geq \sum_{i,j} \mathbf{C}_{i,j} \mathbf{S}'_{i,j} \left(1 + \log \frac{\mathbf{S}_{i,j}}{\mathbf{S}'_{i,j}} \right), \quad (23c)$$

$$\operatorname{tr}(\mathbf{S}^T \mathbf{D}) \leq \sum_{i,j} \mathbf{D}_{i,j} \frac{\mathbf{S}_{i,j}^2 + \mathbf{S}'_{i,j}^2}{2\mathbf{S}'_{i,j}}. \quad (23d)$$

Moreover, all the equalities hold when $\mathbf{S} = \mathbf{S}'$.

See the proofs of those inequalities at Appendix B. According to Proposition 1, Lemma 2 can be easily proved. To find the minimum of Eq. (21), we take

$$\begin{aligned} \frac{\partial f_s(\mathbf{S}_{i,j}, \mathbf{S}'_{i,j})}{\partial \mathbf{S}_{i,j}} &= \frac{2(\mathbf{AS}')_{i,j} \mathbf{S}_{i,j}}{\mathbf{S}'_{i,j}} - \frac{(\mathbf{BS}')_{i,j} \mathbf{S}'_{i,j}}{\mathbf{S}_{i,j}} \\ &\quad - \frac{(\mathbf{B}^\top \mathbf{S}')_{i,j} \mathbf{S}'_{i,j}}{\mathbf{S}_{i,j}} + \mathbf{D}_{i,j} \frac{\mathbf{S}_{i,j}}{\mathbf{S}'_{i,j}} - \mathbf{C}_{i,j} \frac{\mathbf{S}'_{i,j}}{\mathbf{S}_{i,j}}. \end{aligned} \quad (24)$$

Note that the calculation of those derivatives can be found at Appendix B. Moreover, the Hessian matrix containing the second order derivatives

$$\begin{aligned} \frac{\partial^2 f_s(\mathbf{S}, \mathbf{S}')}{\mathbf{S}_{i,j} \mathbf{S}_{l,k}} &= \delta_{il} \delta_{jk} \frac{2(\mathbf{AS}')_{i,j} + \mathbf{D}_{i,j}}{\mathbf{S}'_{i,j}} \\ &\quad + \delta_{il} \delta_{jk} \frac{2(\mathbf{BS}')_{i,j} \mathbf{S}'_{i,j} + \mathbf{C}_{i,j} \mathbf{S}'_{i,j}}{\mathbf{S}_{i,j}^2} \end{aligned} \quad (25)$$

is a diagonal matrix with each element no less than 0, where $\delta_{i,j}$ is a delta function, i.e.,

$$\delta_{i,j} = \begin{cases} 1, & \text{if } i = j, \\ 0, & \text{if } i \neq j. \end{cases} \quad (26)$$

Therefore, Eq. (21) is a convex function, where we can get its global minimization by setting $\frac{\partial f_s(\mathbf{S}, \mathbf{S}')}{\partial \mathbf{S}_{i,j}} = 0$, i.e.,

$$\begin{aligned} \mathbf{S}_{ij} &= \mathbf{S}'_{ij} \sqrt{\frac{\mathbf{C}_{ij} + 2(\mathbf{BS}')_{ij}}{2(\mathbf{AS}')_{ij} + \mathbf{D}_{ij}}} = \\ &\quad \mathbf{S}'_{ij} \sqrt{\frac{(\mathbf{V}\mathbf{V}^\top + \beta\mathbf{W} + \alpha(\mathbf{X}^\top \mathbf{X})^+ + \alpha(\mathbf{X}^\top \mathbf{X})^- \mathbf{S})_{ij}}{(\mathbf{S} + \beta\mathbf{S} + \alpha(\mathbf{X}^\top \mathbf{X})^+ \mathbf{S} + \alpha(\mathbf{X}^\top \mathbf{X})^-)_{ij}}}, \end{aligned} \quad (27)$$

which is exactly the same as Eq. (14). Accordingly, we can conclude that the S-step decreases the objective function of Eq. (10) according to Lemma 1.

Proof of Lemma 3: Lemma 3 can be proved based on the following 2 inequalities.

Proposition 2 For any positive matrices $\mathbf{V} > 0$, $\mathbf{S} > 0$ and $\mathbf{S}' > 0$, the following equations hold:

$$\text{Tr}(\mathbf{V}\mathbf{V}^\top \mathbf{V}\mathbf{V}^\top) \leq \sum_{ij} \sum_{k=1}^c (\mathbf{V}^t \mathbf{V}^{t\top})_{ij} \mathbf{V}_{ik}^t \times \frac{\mathbf{V}_{jk}^4}{\mathbf{V}_{jk}^{t^3}}, \quad (28a)$$

$$\text{Tr}(-\mathbf{S}\mathbf{V}\mathbf{V}^\top) \leq -\sum_{ij} \sum_{k=1}^c \mathbf{S}_{ij} \mathbf{V}_{ik}^t \mathbf{V}_{jk}^t \left(1 + \log \frac{\mathbf{V}_{ik} \mathbf{V}_{jk}}{\mathbf{V}_{ik}^t \mathbf{V}_{jk}^t}\right). \quad (28b)$$

Moreover, all the equalities hold when $\mathbf{V} = \mathbf{V}'$.

See the proof of Proposition 2 at Appendix C. Accordingly, Lemma 3 is proved based on Proposition 2. Let's take

$$\begin{aligned} \frac{\partial f_v(\mathbf{V}, \mathbf{V}')}{\partial \mathbf{V}_{j,k}} &= -2 \frac{(\mathbf{S}\mathbf{V}')_{jk} \mathbf{V}'_{jk}}{\mathbf{V}_{jk}} - 2 \frac{(\mathbf{S}^\top \mathbf{V}')_{jk} \mathbf{V}'_{jk}}{\mathbf{V}_{jk}} \\ &\quad + 4 \left(\mathbf{V}' \mathbf{V}'^\top \mathbf{V}' \right)_{jk} \frac{\mathbf{V}_{jk}^3}{\mathbf{V}_{jk}'} \end{aligned} \quad (29)$$

Its Hessian matrix is also a positive diagonal matrix with

$$\begin{aligned} \frac{\partial^2 f_v(\mathbf{V}, \mathbf{V}')}{\partial \mathbf{V}_{j,k} \partial \mathbf{V}_{il}} &= 12 \delta_{ji} \delta_{kl} \left(\mathbf{V}' \mathbf{V}'^\top \mathbf{V}' \right)_{jk} \frac{\mathbf{V}_{jk}^3}{\mathbf{V}_{jk}'} \\ &\quad + 2 \delta_{ji} \delta_{kl} \frac{(\mathbf{S}\mathbf{V}')_{jk} \mathbf{V}'_{jk}}{\mathbf{V}_{jk}^2} + 2 \delta_{ji} \delta_{kl} \frac{(\mathbf{S}^\top \mathbf{V}')_{jk} \mathbf{V}'_{jk}}{\mathbf{V}_{jk}^2}. \end{aligned} \quad (30)$$

Therefore, $f_v(\mathbf{V}, \mathbf{V}')$ is convex w.r.t. \mathbf{V}_{jk} . Let $\frac{\partial g(\mathbf{V}, \mathbf{V}')}{\partial \mathbf{V}_{j,k}} = 0$, we get the minimum of $f_v(\mathbf{V}, \mathbf{V}')$ at

$$\mathbf{V}_{jk} = \mathbf{V}'_{jk} \times \sqrt[4]{\frac{(\mathbf{S}\mathbf{V}')_{jk} + (\mathbf{S}^\top \mathbf{V}')_{jk}}{2(\mathbf{V}' \mathbf{V}'^\top \mathbf{V}')_{jk}}} \quad (31)$$

which is exactly the same as Eq. (15). Accordingly, we can conclude that the V-step decreases the objective function of Eq. (10) according to Lemma 1. Combining with Lemma 2, we can conclude that each optimization step can decrease the objective function of Eq. (10). In addition, Eq. (10) is lower-bounded, thus Algorithm is locally convergent. The proof of Theorem 1-1) is complete.

B. Proof of Theorem 1-2

Recall the Lagrangian function of Eq. (10) in Eq. (11), its KKT conditions [46] are summarized as

$$\begin{cases} \mathbf{S} \geq 0, \\ \mathbf{V} \geq 0, \\ \Phi \geq 0, \\ \Psi \geq 0, \\ \Phi_{ij} \mathbf{S}_{ij} = 0, \forall i, j, \\ \Psi_{ij} \mathbf{V}_{ij} = 0, \forall i, j, \\ \frac{\partial \mathcal{L}}{\partial \mathbf{S}} = 0, \\ \frac{\partial \mathcal{L}}{\partial \mathbf{V}} = 0. \end{cases} \quad (32)$$

Let's first prove the KKT conditions related to \mathbf{S} hold. Without loss of generality, assume \mathbf{S} is initialized with a positive matrix, i.e., $\mathbf{S}^0 > 0$, and $\{\mathbf{S}^t\}_{t=0}^{+\infty}$ converges to \mathbf{S}^* . At convergence, we have either $\mathbf{S}_{ij}^* > 0$ or $\mathbf{S}_{ij}^* = 0$.

When $\mathbf{S}_{ij}^* = 0$, we have

$$\begin{aligned} 0 = \mathbf{S}_{ij}^* &= \lim_{t \rightarrow \infty} \mathbf{S}_{ij}^t = \mathbf{S}_{ij}^0 \times \\ &\quad \lim_{t \rightarrow \infty} \prod_{r=1}^t \sqrt{\frac{(\mathbf{V}\mathbf{V}^\top + \beta\mathbf{W} + \alpha(\mathbf{X}^\top \mathbf{X})^+ + \alpha(\mathbf{X}^\top \mathbf{X})^- \mathbf{S}^r)_{ij}}{(\mathbf{S}^r + \beta\mathbf{S}^r + \alpha(\mathbf{X}^\top \mathbf{X})^+ \mathbf{S}^r + \alpha(\mathbf{X}^\top \mathbf{X})^-)_{ij}}}. \end{aligned} \quad (33)$$

Accordingly, we have

$$\lim_{t \rightarrow \infty} \frac{(\mathbf{V}\mathbf{V}^\top + \beta\mathbf{W} + \alpha(\mathbf{X}^\top \mathbf{X})^+ + \alpha(\mathbf{X}^\top \mathbf{X})^- \mathbf{S}^t)_{ij}}{(\mathbf{S}^t + \beta\mathbf{S}^t + \alpha(\mathbf{X}^\top \mathbf{X})^+ \mathbf{S}^t + \alpha(\mathbf{X}^\top \mathbf{X})^-)_{ij}} < 1, \quad (34)$$

which equals to

$$\left(\mathbf{V}\mathbf{V}^\top + \alpha \mathbf{X}^\top \mathbf{X} + \beta \mathbf{W} \right)_{ij} < (\mathbf{S}^* + \alpha \mathbf{X}^\top \mathbf{X} \mathbf{S}^* + \beta \mathbf{S}^*)_{ij}. \quad (35)$$

Consequently, we have

$$\begin{aligned} \Phi_{ij}^* &= (\mathbf{S}^* + \alpha \mathbf{X}^\top \mathbf{X} \mathbf{S}^* + \beta \mathbf{S}^*)_{ij} \\ &\quad - \left(\mathbf{V} \mathbf{V}^\top + \alpha \mathbf{X}^\top \mathbf{X} + \beta \mathbf{W} \right)_{ij} > 0. \end{aligned} \quad (36)$$

When $\mathbf{S}_{ij}^* > 0$, at convergence we have

$$\mathbf{S}_{ij}^* = \mathbf{S}_{ij}^* \sqrt{\left(\frac{\mathbf{V} \mathbf{V}^\top + \beta \mathbf{W} + \alpha (\mathbf{X}^\top \mathbf{X})^+ + \alpha (\mathbf{X}^\top \mathbf{X})^- \mathbf{S}^*}{\mathbf{S}^* + \beta \mathbf{S}^* + \alpha (\mathbf{X}^\top \mathbf{X})^+ \mathbf{S}^* + \alpha (\mathbf{X}^\top \mathbf{X})^-} \right)_{ij}}. \quad (37)$$

Hence,

$$\left(\mathbf{V} \mathbf{V}^\top + \alpha \mathbf{X}^\top \mathbf{X} + \beta \mathbf{W} \right)_{ij} = (\mathbf{S}^* + \alpha \mathbf{X}^\top \mathbf{X} \mathbf{S}^* + \beta \mathbf{S}^*)_{ij}. \quad (38)$$

As a result,

$$\Phi_{ij}^* = (\mathbf{S}^* + \alpha \mathbf{X}^\top \mathbf{X} \mathbf{S}^* + \beta \mathbf{S}^*)_{ij} - \left(\mathbf{V} \mathbf{V}^\top + \alpha \mathbf{X}^\top \mathbf{X} + \beta \mathbf{W} \right)_{ij} = 0. \quad (39)$$

Based on the above analysis, we can conclude that the following conditions hold:

$$\begin{cases} \mathbf{S} \geq 0, \\ \Phi \geq 0, \\ \Phi_{ij} \mathbf{S}_{ij} = 0, \forall i, j, \\ \frac{\partial \mathcal{L}}{\partial \mathbf{S}} = 0. \end{cases} \quad (40)$$

With the same pipeline, we can prove the following conditions related to \mathbf{V} also hold:

$$\begin{cases} \mathbf{V} \geq 0, \\ \Psi \geq 0, \\ \Psi_{ij} \mathbf{V}_{ij} = 0, \forall i, j, \\ \frac{\partial \mathcal{L}}{(\partial \mathbf{V})_{i,j}} = 0, \forall i, j. \end{cases} \quad (41)$$

Combining Eqs. (40) and (41) together, the proof of Theorem 1-2 is complete.

C. Proof of Theorem 1-3

When initialized with positive matrices, both Eqs. (15) and (14) just consist of operations like multiplication, addition and division of nonnegative matrices. Thus, the non-negativity of both \mathbf{S} and \mathbf{V} are guaranteed in each iteration.

Moreover, when \mathbf{S} is initialized with an off-diagonal matrix, i.e., $\text{diag}(\mathbf{S}) = 0$, at each iteration \mathbf{S}_{ii} is updated as

$$\mathbf{S}_{ii}^t = \mathbf{S}_{ii}^{t-1} \sqrt{\left(\frac{\mathbf{V} \mathbf{V}^\top + \beta \mathbf{W} + \alpha (\mathbf{X}^\top \mathbf{X})^+ + \alpha (\mathbf{X}^\top \mathbf{X})^- \mathbf{S}^t}{\mathbf{S}^{t-1} + \beta \mathbf{S}^{t-1} + \alpha (\mathbf{X}^\top \mathbf{X})^+ \mathbf{S}^{t-1} + \alpha (\mathbf{X}^\top \mathbf{X})^-} \right)_{ii}}, \quad (42)$$

where we can recursively obtain that

$$\begin{aligned} \mathbf{S}_{ii}^{t+1} &= \mathbf{S}_{ii}^0 \sqrt{\left(\frac{\mathbf{V} \mathbf{V}^\top + \beta \mathbf{W} + \alpha (\mathbf{X}^\top \mathbf{X})^+ + \alpha (\mathbf{X}^\top \mathbf{X})^- \mathbf{S}^0}{\mathbf{S}^0 + \beta \mathbf{S}^0 + \alpha (\mathbf{X}^\top \mathbf{X})^+ \mathbf{S}^0 + \alpha (\mathbf{X}^\top \mathbf{X})^-} \right)_{ii}} \\ &\quad \times \prod_{\tau=1}^t \mathbf{S}_{ii}^\tau \sqrt{\left(\frac{\mathbf{V} \mathbf{V}^\top + \beta \mathbf{W} + \alpha (\mathbf{X}^\top \mathbf{X})^+ + \alpha (\mathbf{X}^\top \mathbf{X})^- \mathbf{S}^\tau}{\mathbf{S}^\tau + \beta \mathbf{S}^\tau + \alpha (\mathbf{X}^\top \mathbf{X})^+ \mathbf{S}^\tau + \alpha (\mathbf{X}^\top \mathbf{X})^-} \right)_{ii}}. \end{aligned} \quad (43)$$

Since $\mathbf{S}_{ii}^0 = 0, \forall i$, at each iteration $\text{diag}(\mathbf{S}^t) = 0$ holds. The proof of Theorem 1-3 is complete, and our algorithm can remove the trivial solution naturally.

APPENDIX B

PROOF OF PROPOSITION 1 AND CORRESPONDING DERIVATIVE

The proof of Eq. (23a): Let $\mathbf{S}_{ij} = u_{ij} \mathbf{S}'_{ij}$ and $u_{ij} > 0, \forall i, j$, we have

$$\begin{aligned} &\sum_{i,j} \frac{(\mathbf{A} \mathbf{S}')_{i,j} \mathbf{S}_{i,j}^2}{\mathbf{S}'_{i,j}} - \text{tr}(\mathbf{S}^\top \mathbf{A} \mathbf{S}) \\ &= \sum_{ijk} \mathbf{A}_{ik} \mathbf{S}'_{kj} \mathbf{S}'_{ij} u_{ij}^2 - \sum_{ijk} \mathbf{A}_{ik} \mathbf{S}'_{kj} \mathbf{S}'_{ij} u_{ij} u_{kj} = \Delta \end{aligned} \quad (44)$$

Since \mathbf{A} is a symmetric matrix, we can exchange the indicator (ik) in Eq. (44) and get

$$\Delta = \sum_{ijk} \mathbf{A}_{ik} \mathbf{S}'_{kj} \mathbf{S}'_{ij} u_{kj}^2 - \sum_{ijk} \mathbf{A}_{ik} \mathbf{S}'_{kj} \mathbf{S}'_{ij} u_{ij} u_{kj}. \quad (45)$$

Combining Eq. (44) and Eq. (45) together, we have

$$\Delta = \frac{1}{2} \sum_{ijk} \mathbf{A}_{ik} \mathbf{S}'_{kj} \mathbf{S}'_{ij} (u_{kj}^2 + u_{ij}^2 - 2u_{ij} u_{kj}) \geq 0 \quad (46)$$

Thus, Eq. (23a) holds. Moreover, the derivative of $\sum_{i,j} \frac{(\mathbf{A} \mathbf{S}')_{i,j} \mathbf{S}_{i,j}^2}{\mathbf{S}'_{i,j}}$ w.r.t. \mathbf{S}_{ij} is

$$\frac{\partial \sum_{i,j} \frac{(\mathbf{A} \mathbf{S}')_{i,j} \mathbf{S}_{i,j}^2}{\mathbf{S}'_{i,j}}}{\partial \mathbf{S}_{ij}} = 2 \frac{(\mathbf{A} \mathbf{S}')_{i,j} \mathbf{S}_{i,j}}{\mathbf{S}'_{i,j}}. \quad (47)$$

The proof of Eq. (23b):

$$\begin{aligned} &\text{tr}(\mathbf{S}^\top \mathbf{B} \mathbf{S}) - \sum_{ijk} \mathbf{B}_{jk} \mathbf{S}'_{ki} \mathbf{S}'_{ji} \left(1 + \log \frac{\mathbf{S}_{ki} \mathbf{S}_{ji}}{\mathbf{S}'_{ki} \mathbf{S}'_{ji}} \right) = \\ &\sum_{ijk} \mathbf{B}_{jk} \mathbf{S}_{ki} \mathbf{S}_{ji} - \sum_{ijk} \mathbf{B}_{jk} \mathbf{S}'_{ki} \mathbf{S}'_{ji} \left(1 + \log \frac{\mathbf{S}_{ki} \mathbf{S}_{ji}}{\mathbf{S}'_{ki} \mathbf{S}'_{ji}} \right). \end{aligned} \quad (48)$$

According to the inequality $x > 1 + \log(x), \forall x > 0$, and let $x = \frac{\mathbf{S}_{ki} \mathbf{S}_{ji}}{\mathbf{S}'_{ki} \mathbf{S}'_{ji}}$, we can prove Eq. (48) ≥ 0 holds and likewise Eq. (23b).

Let $f = \sum_{ijk} \mathbf{B}_{jk} \mathbf{S}'_{ki} \mathbf{S}'_{ji} \left(1 + \log \frac{\mathbf{S}_{ki} \mathbf{S}_{ji}}{\mathbf{S}'_{ki} \mathbf{S}'_{ji}} \right) \propto \sum_{ijk} \mathbf{B}_{jk} \mathbf{S}'_{ki} \mathbf{S}'_{ji} (\log \mathbf{S}_{ki} + \log \mathbf{S}_{ji})$, to calculate the derivate, let $f_1 = \sum_{ijk} \mathbf{B}_{jk} \mathbf{S}'_{ki} \mathbf{S}'_{ji} (\log \mathbf{S}_{ki})$ and $f_2 = \sum_{ijk} \mathbf{B}_{jk} \mathbf{S}'_{ki} \mathbf{S}'_{ji} (\log \mathbf{S}_{ji})$. Particularly, exchanging i with j in f_1 , we have $f_1 = \sum_{ijk} \mathbf{B}_{ik} \mathbf{S}'_{kj} \mathbf{S}'_{ij} (\log \mathbf{S}_{kj})$. Then exchanging i and k , we have $f_1 = \sum_{ijk} \mathbf{B}_{ki} \mathbf{S}'_{ij} \mathbf{S}'_{kj} (\log \mathbf{S}_{ij})$. Accordingly,

$$\frac{\partial f_1}{\partial \mathbf{S}_{i,j}} = \frac{\mathbf{B}_{ki} \mathbf{S}'_{kj} \mathbf{S}'_{ij}}{\mathbf{S}_{i,j}} = \frac{(\mathbf{B}^\top \mathbf{S}')_{i,j} \mathbf{S}'_{ij}}{\mathbf{S}_{i,j}}. \quad (49)$$

Exchanging i with j in f_2 , we have $f_2 = \sum_{ijk} \mathbf{B}_{ik} \mathbf{S}'_{kj} \mathbf{S}'_{ij} (\log \mathbf{S}_{ij})$. Accordingly,

$$\frac{\partial f_2}{\partial \mathbf{S}_{i,j}} = \frac{\mathbf{B}_{ik} \mathbf{S}'_{kj} \mathbf{S}'_{ij}}{\mathbf{S}_{i,j}} = \frac{(\mathbf{B} \mathbf{S}')_{i,j} \mathbf{S}'_{ij}}{\mathbf{S}_{i,j}}. \quad (50)$$

Finally, we the corresponding derivate is

$$\frac{\partial f}{\partial \mathbf{S}_{i,j}} = \frac{(\mathbf{B} \mathbf{S}')_{i,j} \mathbf{S}'_{i,j}}{\mathbf{S}_{i,j}} + \frac{(\mathbf{B}^\top \mathbf{S}')_{i,j} \mathbf{S}'_{i,j}}{\mathbf{S}_{i,j}}. \quad (51)$$

The proof of Eq. (23c):

$$\begin{aligned} \text{tr}(\mathbf{S}^T \mathbf{C}) - \sum_{i,j} \mathbf{C}_{i,j} \mathbf{S}'_{i,j} \left(1 + \log \frac{\mathbf{S}_{i,j}}{\mathbf{S}'_{i,j}} \right) \\ = \sum_{i,j} \mathbf{C}_{i,j} \mathbf{S}_{i,j} - \sum_{i,j} \mathbf{C}_{i,j} \mathbf{S}'_{i,j} \left(1 + \log \frac{\mathbf{S}_{i,j}}{\mathbf{S}'_{i,j}} \right). \end{aligned} \quad (52)$$

According to inequality $x > 1 + \log(x), \forall x > 0$, and let $x = \frac{\mathbf{S}_{i,j}}{\mathbf{S}'_{i,j}}$, we can prove Eq. (52) ≥ 0 holds and likewise Eq. (23c). The corresponding derivative is calculated as

$$\frac{\partial \sum_{i,j} \mathbf{C}_{i,j} \mathbf{S}'_{i,j} \left(1 + \log \frac{\mathbf{S}_{i,j}}{\mathbf{S}'_{i,j}} \right)}{\partial \mathbf{S}_{i,j}} = \mathbf{C}_{i,j} \frac{\mathbf{S}'_{i,j}}{\mathbf{S}_{i,j}}. \quad (53)$$

The proof of Eq. (23d):

$$\begin{aligned} \text{tr}(\mathbf{S}^T \mathbf{D}) - \sum_{i,j} \mathbf{D}_{i,j} \frac{\mathbf{S}_{i,j}^2 + \mathbf{S}'_{i,j}{}^2}{2\mathbf{S}'_{i,j}} \\ = \sum_{i,j} \mathbf{S}_{i,j} \mathbf{D}_{i,j} - \sum_{i,j} \mathbf{D}_{i,j} \frac{\mathbf{S}_{i,j}^2 + \mathbf{S}'_{i,j}{}^2}{2\mathbf{S}'_{i,j}}. \end{aligned} \quad (54)$$

According to the Janson inequality $a^2 + b^2 - 2ab \geq 0, \forall a, b$, and let $a = \mathbf{S}_{i,j}, b = \mathbf{S}'_{i,j}$, we can prove Eq. (54) ≤ 0 holds and likewise Eq. (23d). The corresponding derivative is calculated as

$$\frac{\partial \sum_{i,j} \mathbf{D}_{i,j} \frac{\mathbf{S}_{i,j}^2 + \mathbf{S}'_{i,j}{}^2}{2\mathbf{S}'_{i,j}}}{\partial \mathbf{S}_{i,j}} = \mathbf{D}_{i,j} \frac{\mathbf{S}_{i,j}}{\mathbf{S}'_{i,j}}. \quad (55)$$

APPENDIX C

PROOF OF PROPOSITION 2 AND CORRESPONDING DERIVATIVE

The proof of Eq. (28a):

Let $\mathbf{V}_{ij} = u_{ij} \mathbf{V}'_{ij}$ and $u_{ij} > 0, \forall i, j$, and $u_{ij} > 0$, we have

$$\begin{aligned} \sum_{i,j} \sum_{k=1}^c (\mathbf{V}' \mathbf{V}'^T)_{i,j} \mathbf{V}'_{ik} \times \frac{\mathbf{V}_{jk}^4}{\mathbf{V}'_{jk}^3} - \text{Tr}(\mathbf{V} \mathbf{V}^T \mathbf{V} \mathbf{V}^T) \\ = \sum_{i,j} \sum_{kl} \mathbf{V}'_{il} \mathbf{V}'_{jl} \mathbf{V}'_{ik} \mathbf{V}'_{jl} u_{il} u_{jl} u_{ik}^4 u_{jk} \\ - \sum_{i,j} \sum_{kl} \mathbf{V}'_{il} \mathbf{V}'_{jl} \mathbf{V}'_{ik} \mathbf{V}'_{jl} u_{il} u_{jl} u_{ik} u_{jk} = \Delta. \end{aligned} \quad (56)$$

Denote $\gamma = \sum_{i,j} \sum_{kl} \mathbf{V}'_{il} \mathbf{V}'_{jl} \mathbf{V}'_{ik} \mathbf{V}'_{jl} u_{il} u_{jl} u_{ik} u_{jk}$, exchanging the indicators i and j in Eq. (56), we have

$$\Delta = \sum_{i,j} \sum_{kl} \mathbf{V}'_{il} \mathbf{V}'_{jl} \mathbf{V}'_{ik} \mathbf{V}'_{jk} u_{ik}^4 - \gamma. \quad (57)$$

Exchanging the indicators k and l in Eq. (56), we have

$$\Delta = \sum_{i,j} \sum_{kl} \mathbf{V}'_{il} \mathbf{V}'_{jl} \mathbf{V}'_{ik} \mathbf{V}'_{jk} u_{il}^4 - \gamma. \quad (58)$$

Exchanging the indicators ik and jl in Eq. (56), we have

$$\Delta = \sum_{i,j} \sum_{kl} \mathbf{V}'_{il} \mathbf{V}'_{jl} \mathbf{V}'_{ik} \mathbf{V}'_{jk} u_{jl}^4 - \gamma. \quad (59)$$

Combining Eqs (56)-(59) together, we have

$$\begin{aligned} \Delta = \sum_{i,j} \sum_{kl} \mathbf{V}'_{il} \mathbf{V}'_{jl} \mathbf{V}'_{ik} \mathbf{V}'_{jk} \left(\frac{u_{il}^4 + u_{jl}^4 + u_{ik}^4 + u_{jk}^4}{4} \right. \\ \left. - u_{il} u_{jl} u_{ik} u_{jk} \right) \geq \sum_{i,j} \sum_{kl} \mathbf{V}'_{il} \mathbf{V}'_{jl} \mathbf{V}'_{ik} \mathbf{V}'_{jk} \times \\ \left(\frac{u_{il}^2 u_{jl}^2 + u_{ik}^2 u_{jk}^2}{2} - u_{il} u_{jl} u_{ik} u_{jk} \right) \geq 0 \end{aligned} \quad (60)$$

The proof of Eq. (28a) is completed. For the corresponding derivate, we have

$$\frac{\partial \sum_{i,j} \sum_{k=1}^c (\mathbf{V}' \mathbf{V}'^T)_{i,j} \mathbf{V}'_{ik} \times \frac{\mathbf{V}_{jk}^4}{\mathbf{V}'_{jk}^3}}{\partial \mathbf{V}_{jk}} = 4 (\mathbf{V}' \mathbf{V}'^T)_{i,j} \mathbf{V}'_{ik} \mathbf{V}_{jk}^3. \quad (61)$$

The proof of Eq. (28b)

The proof of Eq. (28b) is equivalent to the proof of Eq. (23b).

REFERENCES

- [1] Z. Wu and R. Leahy, "An optimal graph theoretic approach to data clustering: Theory and its application to image segmentation," *IEEE transactions on pattern analysis and machine intelligence*, vol. 15, no. 11, pp. 1101–1113, 1993.
- [2] K.-S. Chuang, H.-L. Tzeng, S. Chen, J. Wu, and T.-J. Chen, "Fuzzy c-means clustering with spatial information for image segmentation," *computerized medical imaging and graphics*, vol. 30, no. 1, pp. 9–15, 2006.
- [3] W. Wu, Y. Jia, S. Kwong, and J. Hou, "Pairwise constraint propagation-induced symmetric nonnegative matrix factorization," *IEEE Transactions on Neural Networks and Learning Systems*, vol. 29, no. 12, pp. 6348–6361, Dec 2018.
- [4] W. Wu, S. Kwong, Y. Zhou, Y. Jia, and W. Gao, "Nonnegative matrix factorization with mixed hypergraph regularization for community detection," *Information Sciences*, vol. 435, pp. 263–281, 2018.
- [5] J. Das, P. Mukherjee, S. Majumder, and P. Gupta, "Clustering-based recommender system using principles of voting theory," in *Contemporary computing and informatics (IC3I), 2014 international conference on*. IEEE, 2014, pp. 230–235.
- [6] Z. Yu, H. Chen, J. You, H.-S. Wong, J. Liu, L. Li, and G. Han, "Double selection based semi-supervised clustering ensemble for tumor clustering from gene expression profiles," *IEEE/ACM Transactions on Computational Biology and Bioinformatics (TCBB)*, vol. 11, no. 4, pp. 727–740, 2014.
- [7] Z. Yu, L. Li, J. You, H.-S. Wong, and G. Han, "Sc³: Triple spectral clustering-based consensus clustering framework for class discovery from cancer gene expression profiles," *IEEE/ACM Transactions on Computational Biology and Bioinformatics*, vol. 9, no. 6, pp. 1751–1765, 2012.
- [8] Z. Yu, H.-S. Wong, and H. Wang, "Graph-based consensus clustering for class discovery from gene expression data," *Bioinformatics*, vol. 23, no. 21, pp. 2888–2896, 2007.
- [9] A. N. Gorban, B. Kégl, D. C. Wunsch, A. Y. Zinovyev *et al.*, *Principal manifolds for data visualization and dimension reduction*. Springer, 2008, vol. 58.
- [10] B. Jian and B. C. Vemuri, "Robust point set registration using gaussian mixture models," *IEEE transactions on pattern analysis and machine intelligence*, vol. 33, no. 8, pp. 1633–1645, 2011.
- [11] D. Comaniciu and P. Meer, "Mean shift: A robust approach toward feature space analysis," *IEEE Transactions on Pattern Analysis & Machine Intelligence*, no. 5, pp. 603–619, 2002.
- [12] Y. Cheng, "Mean shift, mode seeking, and clustering," *IEEE transactions on pattern analysis and machine intelligence*, vol. 17, no. 8, pp. 790–799, 1995.
- [13] A. Y. Ng, M. I. Jordan, and Y. Weiss, "On spectral clustering: Analysis and an algorithm," in *Advances in neural information processing systems*, 2002, pp. 849–856.
- [14] Y. Yang, H. T. Shen, F. Nie, R. Ji, and X. Zhou, "Nonnegative spectral clustering with discriminative regularization," in *Twenty-Fifth AAAI Conference on Artificial Intelligence*, 2011.

- [15] D. Kuang, S. Yun, and H. Park, "Symnmf: nonnegative low-rank approximation of a similarity matrix for graph clustering," *Journal of Global Optimization*, vol. 62, no. 3, pp. 545–574, 2015.
- [16] D. Kuang, C. Ding, and H. Park, "Symmetric nonnegative matrix factorization for graph clustering," in *Proceedings of the 2012 SIAM international conference on data mining*. SIAM, 2012, pp. 106–117.
- [17] L. Zelnik-Manor and P. Perona, "Self-tuning spectral clustering," in *Advances in neural information processing systems*, 2005, pp. 1601–1608.
- [18] U. Von Luxburg, "A tutorial on spectral clustering," *Statistics and computing*, vol. 17, no. 4, pp. 395–416, 2007.
- [19] B. Cheng, J. Yang, S. Yan, Y. Fu, and T. S. Huang, "Learning with ℓ^1 -graph for image analysis," *IEEE Transactions on Image Processing*, vol. 19, no. 4, pp. 858–866, April 2010.
- [20] G. Liu, Z. Lin, and Y. Yu, "Robust subspace segmentation by low-rank representation," in *Proceedings of the 27th international conference on machine learning (ICML-10)*, 2010, pp. 663–670.
- [21] E. Elhamifar and R. Vidal, "Sparse subspace clustering," in *2009 IEEE Conference on Computer Vision and Pattern Recognition*. IEEE, 2009, pp. 2790–2797.
- [22] X. Peng, Z. Yu, Z. Yi, and H. Tang, "Constructing the l2-graph for robust subspace learning and subspace clustering," *IEEE transactions on cybernetics*, vol. 47, no. 4, pp. 1053–1066, 2017.
- [23] F. Nie, X. Wang, and H. Huang, "Clustering and projected clustering with adaptive neighbors," in *Proceedings of the 20th ACM SIGKDD international conference on Knowledge discovery and data mining*. ACM, 2014, pp. 977–986.
- [24] X. Dong, D. Thanou, P. Frossard, and P. Vandergheynst, "Learning laplacian matrix in smooth graph signal representations," *IEEE Transactions on Signal Processing*, vol. 64, no. 23, pp. 6160–6173, 2016.
- [25] C.-G. Li, C. You, and R. Vidal, "Structured sparse subspace clustering: A joint affinity learning and subspace clustering framework," *IEEE Trans. Image Processing*, vol. 26, no. 6, pp. 2988–3001, 2017.
- [26] C.-G. Li, Z. Lin, H. Zhang, and J. Guo, "Learning semi-supervised representation towards a unified optimization framework for semi-supervised learning," in *Proceedings of the IEEE International Conference on Computer Vision*, 2015, pp. 2767–2775.
- [27] X. Fang, Y. Xu, X. Li, Z. Lai, and W. K. Wong, "Robust semi-supervised subspace clustering via non-negative low-rank representation," *IEEE transactions on cybernetics*, vol. 46, no. 8, pp. 1828–1838, 2016.
- [28] Z. Lai, D. Mo, J. Wen, L. Shen, and W. Wong, "Generalized robust regression for jointly sparse subspace learning," *IEEE Transactions on Circuits and Systems for Video Technology*, 2018.
- [29] Z. Zhang, Y. Zhang, G. Liu, J. Tang, S. Yan, and M. Wang, "Joint label prediction based semi-supervised adaptive concept factorization for robust data representation," *IEEE Transactions on Knowledge and Data Engineering*, 2019.
- [30] F. Nie, S. J. Shi, and X. Li, "Semi-supervised learning with auto-weighting feature and adaptive graph," *IEEE Transactions on Knowledge and Data Engineering*, 2019.
- [31] C. Lu, S. Yan, and Z. Lin, "Convex sparse spectral clustering: Single-view to multi-view," *IEEE Transactions on Image Processing*, vol. 25, no. 6, pp. 2833–2843, 2016.
- [32] Y. Jia, S. Kwong, W. Wu, R. Wang, and W. Gao, "Sparse bayesian learning-based kernel poisson regression," *IEEE transactions on cybernetics*, vol. 49, no. 1, p. 56, 2019.
- [33] J. Wright, A. Ganesh, S. Rao, Y. Peng, and Y. Ma, "Robust principal component analysis: Exact recovery of corrupted low-rank matrices via convex optimization," in *Advances in neural information processing systems*, 2009, pp. 2080–2088.
- [34] E. J. Candès, X. Li, Y. Ma, and J. Wright, "Robust principal component analysis?" *Journal of the ACM (JACM)*, vol. 58, no. 3, p. 11, 2011.
- [35] B. Jiang, C. Ding, B. Luo, and J. Tang, "Graph-laplacian pca: Closed-form solution and robustness," in *Proceedings of the IEEE Conference on Computer Vision and Pattern Recognition*, 2013, pp. 3492–3498.
- [36] D. D. Lee and H. S. Seung, "Algorithms for non-negative matrix factorization," in *Advances in neural information processing systems*, 2001, pp. 556–562.
- [37] D. Cai, X. He, J. Han, and T. S. Huang, "Graph regularized nonnegative matrix factorization for data representation," *IEEE transactions on pattern analysis and machine intelligence*, vol. 33, no. 8, pp. 1548–1560, 2011.
- [38] Z. Zhang and K. Zhao, "Low-rank matrix approximation with manifold regularization," *IEEE transactions on pattern analysis and machine intelligence*, vol. 35, no. 7, pp. 1717–1729, 2013.
- [39] N. Shahid, V. Kalofolias, X. Bresson, M. Bronstein, and P. Vandergheynst, "Robust principal component analysis on graphs," in *Proceedings of the IEEE International Conference on Computer Vision*, 2015, pp. 2812–2820.
- [40] G. Liu, Z. Lin, S. Yan, J. Sun, Y. Yu, and Y. Ma, "Robust recovery of subspace structures by low-rank representation," *IEEE transactions on pattern analysis and machine intelligence*, vol. 35, no. 1, pp. 171–184, 2013.
- [41] X. Guo, "Robust subspace segmentation by simultaneously learning data representations and their affinity matrix," in *Proceedings of the 24th International Conference on Artificial Intelligence*. AAAI Press, 2015, pp. 3547–3553.
- [42] D. Cai, X. He, and J. Han, "Document clustering using locality preserving indexing," *IEEE Transactions on Knowledge and Data Engineering*, vol. 17, no. 12, pp. 1624–1637, 2005.
- [43] C. Ding, X. He, and H. D. Simon, "On the equivalence of nonnegative matrix factorization and spectral clustering," in *Proceedings of the 2005 SIAM International Conference on Data Mining*. SIAM, 2005, pp. 606–610.
- [44] C. Ding and X. He, "K-means clustering via principal component analysis," in *Proceedings of the twenty-first international conference on Machine learning*. ACM, 2004, p. 29.
- [45] D. Kong, C. Ding, H. Huang, and F. Nie, "An iterative locally linear embedding algorithm," in *Proceedings of the 29th International Conference on International Conference on Machine Learning*. Omnipress, 2012, pp. 931–938.
- [46] S. Boyd and L. Vandenberghe, *Convex optimization*. Cambridge university press, 2004.